Both local stability and dispersal contribute to metacommunity sensitivity to asynchronous habitat availability (depending on landscape structure and foodweb complexity)

Pablo Moisset de Espanés[1] and Rodrigo Ramos-Jiliberto[2*]

[1]Centro de Biotecnología y Bioingeniería, Universidad de Chile, Chile. E-mail: pmoisset@ing.uchile.cl
[2]GEMA Center for Genomics, Ecology & Environment, Universidad Mayor, Chile. *E-mail: rodrigo.ramos@umayor.cl

Running title: Local stability in trophic metacommunities

Keywords— local stability, metacommunity dynamics, dynamic landscape, intermittent habitats, ecological networks

Type of article: Letter.

Authorship: P.M. de E. and R.R.J. conceived the research. P.M. de E. conducted the simulations. P.M. de E. and R.R.J. wrote the first draft. Both authors contributed to writing the final manuscript.

Data accessibility: No new data were used in this study. Computer codes for simulations are available at https://doi.org/10.5281/zenodo.10014193.

149 **words in the abstract:**, 4801 **words in the main text:**. 58 **references:**. 3 **figures**, no **tables**, and no **text boxes**.

Corresponding author: Rodrigo Ramos-Jiliberto. Camino La Pirámide 5750 Huechuraba, Santiago, Chile. Tel: +56 2 2518 9262, E-mail: rodrigo.ramos@umayor.cl

Abstract

The stability of isolated communities is determined by foodweb complexity. However, it is unclear how local stability interacts with dispersal in multitrophic metacommunities to shape biodiversity patterns. Furthermore, metacommunity dynamics in landscapes with non-trivial and dynamic structures are less understood. We aim to evaluate the influence of local stabilizing factors versus dispersal in determining the sensitivity of metacommunity biodiversity to increasing site availability asynchrony. Additionally, we assess the role of regional foodweb complexity and landscape structure as modulating factors. To achieve these goals, we developed a model based on random matrices for local communities linked by stochastic dispersal over explicit, dynamic landscapes. Both local and regional stabilizing factors determined the sensitivity of metacommunities to landscape asynchrony. Local factors were more influential in landscapes with fewer sites and lower modularity, and in more complex foodwebs. We delve into the mechanisms underlying our results and discuss potential extensions of our study.

INTRODUCTION

During past decades, there have been remarkable advances in the understanding of the interrelationship between ecological stability, species diversity, and ecosystem functioning May (1972); McCann (2000); Allesina and Tang (2012); Hooper et al. (2012); Loreau and De Mazancourt (2013); Rohr et al. (2014). These advances have been mostly reached considering local, closed ecological communities. However, many natural communities are open to regional influences driven by the dispersal of individuals. The advent of the metacommunity concept Leibold et al. (2004) enlarged the scale of analysis, incorporating the connectedness among local communities for understanding the coordinated dynamics of spatially-structured species assemblages that resemble more closely the structure of real ecosystems. Thus, the dynamics of metacommunities are understood as governed by the interplay between local processes, that take place within local communities, and regional ones, at the level of the whole landscape Thompson et al. (2020). In this vein, a central topic is understanding which properties of metacommunities determine biodiversity robustness to ongoing environmental changes.

At a local level, community stability refers to the ability of a community to retain its function and structure after suffering a disturbance. However, there exist many metrics that capture different aspects of community stability (Kéfi et al., 2019). The arrangement and strength of interactions among species determine the stability of communities and the likelihood of species coexistence therein. In particular, the strength of self-limitation is an important stabilizing mechanism that modulates coexistence (Chesson, 2000; Barabás et al., 2017), along with density-dependent interspecific processes (Chesson, 2000). Topological network properties, such as species richness, connectance, modularity, nestedness (Thébault and Fontaine, 2010), and trophic coherence (Johnson et al., 2014) also shape community stability. In a spatially-structured context, the stability of local communities should be

more relevant for biodiversity maintenance in loosely connected metacommunities, where regional influences are minimal (Thompson and Gonzalez, 2017). However, the likelihood of species introductions from neighboring habitats may be influenced by the stability of the destination community, consequently affecting the probability of species integration into a local community after dispersal Lurgi et al. (2014); Hui et al. (2016). Therefore, local stabilizing factors may play a crucial role in shaping the collective functioning of linked communities. However, this particular aspect has received limited attention in previous research (but see Mougi and Kondoh (2016); Gravel et al. (2016); Thompson and Gonzalez (2017)).

Regional processes are governed by the movements of organisms and propagules among local communities. These dispersal movements allow the colonization and recolonization of available and reachable sites, thereby recovering low-density populations (Mouquet and Loreau, 2003). As a consequence, species dispersal over the landscapes tends to foster local species diversity, among-habitat species composition similarity (Thompson et al., 2020), and overall metacommunity stability (Mougi and Kondoh, 2016). The dispersal process at the metacommunity level and its consequences on biodiversity patterns may heavily depend on landscape structure, i.e., the arrangement of links among local sites through which dispersal can occur. For example, choke points with harsh conditions can hamper the dispersal of species between sub-regions of the landscape. Conversely, high connectivity among sites fosters species abundances and reduces regional extinction probability (Arancibia and Morin, 2022). How sites are arranged into the landscape also affects species dynamics and diversity (Holyoak, 2000; Economo and Keitt, 2010). In addition, the relative importance of a specific archetypal metacommunity driving force (e.g., species sorting vs. mass effect) is also influenced by landscape topology (Suzuki and Economo, 2021). Consequently, there has been a recent push toward incorporating explicit landscape representations in the study of metacommunity dynamics (see, for

example, Borthagaray et al. (2014, 2018)).

Most metacommunity models up to date, indeed those that include explicit dynamics of species abundances, assume that local habitat sites maintain their properties essentially constant over time Leibold et al. (2004). This translates into a static structure of localities (number and connectivity of sites) that compose a landscape, as well as a static set of local conditions and resources within each site. However, real spatially-structured systems deviate significantly from these idealizations, as ecosystems often undergo pronounced changes over time in their physical structure and in local biotic and abiotic factors (Chesson and Huntly, 1989; Erős et al., 2012; Aiken and Navarrete, 2014; Brendonck et al., 2017). Canonical examples of dynamic landscapes (i.e. with a time-varying structure) are found in lentic environments within semiarid and Mediterranean regions (e.g. Olmo et al. (2022)), containing temporary habitats that switch between "active" and "inactive" states. In these systems, alterations in local habitat availability are seasonal, albeit partially unpredictable, that is, subjected to a frequent and stochastic disturbance sensu Holyoak et al. (2020). In small-area landscapes, the initiation of active periods at sites often exhibits a strong temporal correlation, as they are typically caused by rainfall events. Conversely, in large-area landscapes, we expect a weaker synchronization in the starting of active periods, due to the spatial variability in weather conditions. Regardless of landscape size, the duration of active periods can greatly vary among sites because it depends on local factors such as pond capacity and drainage. In general, temporal fluctuations in habitat availability are rarely perfectly synchronized among all sites within a landscape. Consequently, the 'active' periods of two specific sites may only partially overlap or not overlap at all. This asynchrony can have a detrimental impact on biodiversity, particularly for active dispersers, as it hinders dispersal between adjacent sites. Nevertheless, moderate levels of asynchrony can also yield positive effects by enhancing rescue and spatial insurance mechanisms Wilcox et al. (2017).

In this study, we assess the role of local stabilizing factors, *LSFs*, (self-limitation, trophic coherence), versus regional stabilizing factors, *RSFs*, (dispersal ability) in shaping the sensitivity of metacommunity biodiversity and biomass to increasing asynchrony in site availability. We evaluate these effects across gradients of both regional foodweb and landscape complexity. To efficiently simulate systems involving these elements, we developed a model that involves a) random spatially-explicit metacommunities embedded in dynamic landscapes containing temporary sites, b) local community dynamics, described as Lotka-Volterra foodweb equations parameterized by linear programming, reaching equilibria instantaneously to avoid explicit population dynamics, c) stochastic dispersal among sites obeying a Markov process.

METHODS

We outline the key steps of our methods; for details, see Appendix S1.

Model: We represent dynamic landscapes as dynamic graphs, i.e. time-varying graphs with node-dynamics (Harary and Gupta, 1997). Our algorithm creates connected modular landscapes with key parameters n_P (number of sites) and F (controlling the level of modularity). A site of a randomly chosen module is designated as *the mainland*. At a given time, each site p is in either of two states: "active" or "inactive." Species can be present in p only when the site is "active." The mainland is always "active", and all species in the regional pool are present therein. All the other sites transition stochastically between the two states. The regional pool of species –and their interactions– is modeled as a foodweb following Klaise and Johnson (2016). Parameter T (foodweb temperature) controls the degree of trophic coherence, a structural property that strongly determines stability in empirical foodwebs (Johnson et al., 2014). Other key parameters are species richness n_S and foodweb connectance C.

We assume that the dynamics of species' biomasses at a site, is governed by Lotka-Volterra type equations and reaches equilibrium instantaneously. For our study, a key parameter is λ, representing the negative of the diagonal entries of the community matrix. Other parameters are automatically computed to ensure the system is feasible and Lyapunov stable. Dispersal is modeled as a continuous time Markov chain. The dispersal events are coupled with the activation and deactivation events of landscape sites, and with the local community dynamics. The *effective rate* of dispersal between sites p and q is the ratio between the dispersal ability $a \in \mathbb{R}^+$ (a free parameter) and the Euclidean distance between p and q. Dispersal of species s is possible only if p and q are active, s is present in p but not in q, and s is either a basal species, or a consumer with at least one of its preys present in q. After each event, the biomasses of all species present in q are set to the equilibrium of the Lotka-Volterra system, taking extinctions into account.

Experimental design: As main predictor variables, we chose T and λ as LSFs, and a as the RSF. Variables T and λ univocally determine local stability, while a is the canonical metacommunity attribute at a regional level. Parameters T and λ were set to 7 evenly spaced values between 0 and 1.2, and 6 evenly spaced values between -1.0 and -1/3, respectively. Parameter a was set to 5 logarithmically-spaced values between 30 and 3000. The predictors' values were chosen based on preliminary tests, that shed light on the range of predictor values that generate noticeable variation in response variables.Regarding landscape parameters, we used $n_P = 25, 50, 100$ and $F = 5, 10, 50, 75$. For foodweb parameters, we used $C = 0.15, 0.2, 0.25$ and $n_S = 30, 45, 60, 75$. We simulated 6 years of metacommunity dynamics and 50 replicates for each point in the parameter space. Because in our model all sites except the mainland are reset every year, longer simulation times are not needed. We define instantaneous species persistence at time t as the ratio between species richness at t and the number of species in the regional pool. We calculate time series for α (average local) and γ (regional) persistence, denoted as $\mathcal{P}_\alpha(t)$ and $\mathcal{P}_\gamma(t)$

respectively. By computing the continuous power mean, we obtain the scalars $\mathcal{P}_\alpha$ and $\mathcal{P}_\gamma$. Following Jost (2007), we calculate beta persistence $\mathcal{P}_\beta$ as $\mathcal{P}_\gamma/\mathcal{P}_\alpha$. We also calculate time series for γ biomass $\mathcal{B}_\gamma(t)$ as the total metacommunity biomass (summed over all sites and species). We define β biomass $\mathcal{B}_\beta(t)$ as the coefficient of variation of local community biomasses over all sites. Then we compute their power means to obtain scalars $\mathcal{B}_\beta$ and $\mathcal{B}_\gamma$. There is no need to obtain $\mathcal{B}_\alpha$ because it is proportional to $\mathcal{B}_\gamma$.

We focus on assessing how landscape asynchrony A affects the response variables ($\mathcal{P}_\alpha$, $\mathcal{P}_\beta$, $\mathcal{P}_\gamma$, $\mathcal{B}_\beta$, and $\mathcal{B}_\gamma$). For a given response variable x we define the *sensitivity of x to an increase in A* from a low value, call it A_L to a high value A_H. We define

$$\mathcal{S}[x] = \frac{x_H - x_L}{A_H - A_L} \tag{1}$$

where x_L and x_H are the values of X for A_L and A_H respectively. In our experiments, we set $A_L = 0$ and $A_H = 0.5$. For brevity, we write *A-sensitivities* to denote the elements of the set $\{\mathcal{S}[\mathcal{P}_\alpha], \mathcal{S}[\mathcal{P}_\beta], \mathcal{S}[\mathcal{P}_\gamma], \mathcal{S}[\mathcal{B}_\beta], \mathcal{S}[\mathcal{B}_\gamma]\}$. We quantified the effects of LSFs versus RSFs on the A-sensitivities. As predictor variables, we used T and λ, which regulate local community stability, and $\hat{a} = \log_{10}(a)$, which regulates regional processes. We also tested all possible quadratic interactions among the three main predictors. Standardized effect sizes were obtained from the coefficients of multiple linear regressions after rescaling the main predictors to z-scores. Also, we tested the possibility of removing some of the predictors by comparing the corrected Akaike information criterion (AICc) values for all linear models nested within our full model.

RESULTS

As a starting point, we analyze how LSFs (T and λ) affect species persistence and community biomass as a result of the assembly process of a single community from the

regional species pool. The assembly process occurs in the context of unlimited access to the species pool, and permanent habitat availability, i.e., the site is always "active." Therefore, community composition is mainly governed by local processes. An analysis of Fig. 1 reveals that both T and λ exerted marked effects on community diversity and biomass. Species persistence $\mathcal{P}$ decreased with T and increased with λ (Fig. 1A). The opposite trend was obtained for community biomass $\mathcal{B}$ (Fig. 1B). Figs. S2 and S3 in Appendix S1 show the influence of foodweb complexity (n_S and C) on $\mathcal{P}$ and $\mathcal{B}$. On one hand, n_S lowered $\mathcal{P}$ in the sense that it shrank the region in the λ, T parameter space where $\mathcal{P}$ is high. On the other hand, n_S increased $\mathcal{B}$. By contrast, C decreased both $\mathcal{P}$ and $\mathcal{B}$.

Next, we extend the experiments to metacommunities in dynamic landscapes. To gain initial insights into the effects of landscape asynchrony A on metacommunity attributes, we run our full model using two dispersal rates. We assessed the relative changes in $\mathcal{P}$ and $\mathcal{B}$ while varying A from 0 to 0.5 As we see in Fig. 2, increasing A reduced both $\mathcal{P}_\alpha$ and $\mathcal{B}_\gamma$, while it increased $\mathcal{P}_\beta$ and $\mathcal{B}_\beta$. The response of $\mathcal{P}_\gamma$ was comparatively smaller and its sign depended on dispersal ability a. In general, increasing a strengthened the effect of A, specially for $\mathcal{P}_\beta$.

Effects of local and regional stabilizing factors: According to the AICc, the full model outperformed all nested, smaller models. Fig. 3 shows the effect sizes of each predictor on A-sensitivities of species persistence.

Dispersal ability $\hat{a}$ was a strong predictor of $\mathcal{S}[\mathcal{P}_\alpha]$, $\mathcal{S}[\mathcal{P}_\beta]$, and $\mathcal{S}[\mathcal{P}_\gamma]$. Moreover, $\hat{a}$ determined A-sensitivities in a nonlinear way, as indicated by the effect sizes of $\hat{a}^2$ (Fig. 3). Increasing $\hat{a}$ tended to reduce $\mathcal{S}[\mathcal{P}_\alpha]$, as indicated by the negative effect sizes. This trend held for metacommunities governed by the three parameter sets: base condition (Fig. 3a), complex foodwebs (Fig. 3d), and scattered/spread landscapes (Fig. 3g). For all the cases in Fig. 3, the effect of $\hat{a}$ over $\mathcal{S}[\mathcal{P}_\beta]$ was parameter (foodweb and landscape) dependent and

highly nonlinear. However, $\hat{a}$ was not the strongest predictor of $\mathcal{S}[\mathcal{P}_\beta]$ for denser/modular landscapes (Fig. 3b,e). For the base case, $\hat{a}$ had a positive and mostly linear effect on $\mathcal{S}[\mathcal{P}_\gamma]$ (Fig. 3c). For complex foodwebs, this effect, although qualitatively the same as for the base case, was not the dominant one (Fig. 3f). For scattered/spread landscapes, the effect of $\hat{a}$ on $\mathcal{S}[\mathcal{P}_\gamma]$, although relatively small, was highly nonlinear (Fig. 3i). Predictors λ and T exerted noticeable effects on all A-sensitivities, except $\mathcal{S}[\mathcal{P}_\beta]$ in scattered landscapes. The effect sizes of λ on persistence-related A-sensitivities were of similar magnitude but, as expected, of opposite sign than those of T. The quadratic terms for λ and T were relatively small. Strengthening local stability, either through increasing λ or decreasing T, led to a decrease in $\mathcal{S}[\mathcal{P}_\alpha]$, and of $\mathcal{S}[\mathcal{P}_\beta]$ (except for scattered landscapes), while it increased $\mathcal{S}[\mathcal{P}_\gamma]$. Interaction effects between $\hat{a}$ and both λ and T were of considerable size for $\mathcal{S}[\mathcal{P}_\gamma]$, and for $\mathcal{S}[\mathcal{P}_\beta]$ (base parameters and complex foodwebs). Predictor $T \times \hat{a}$ increased $\mathcal{S}[\mathcal{B}_\beta]$ while it decreased $\mathcal{S}[\mathcal{B}_\gamma]$. Predictor $\lambda \times \hat{a}$ had the opposite effects.

Effects of landscape structure: The number of sites in the landscape n_P, and the excess factor F, exerted noticeable effects on the relative effect sizes of predictors on A-sensitivities. In general, the absolute sizes of the effects increased with n_P, except on $\mathcal{S}[\mathcal{B}_\beta]$ (Figs. S4-S8). Increases in F tended to decrease the effects exerted by $\hat{a}$ and $\hat{a}^2$ on $\mathcal{S}[\mathcal{P}_\alpha]$. Conversely, for $\mathcal{S}[\mathcal{P}_\gamma]$, these effects sizes had a tendency to be magnified by F. Large n_P values strengthened the effects of F on persistence-related A-sensitivities. The sensitivity $\mathcal{S}[\mathcal{B}_\beta]$ remained almost fully explained by $\hat{a}$ (and $\hat{a}^2$) for all the explored parameter space. Interestingly, for $\mathcal{S}[\mathcal{P}_\gamma]$ the importance of T and λ relative to that of $\hat{a}$ increased for small values of n_P and F.

Effects of foodweb topology: Foodweb parameters C and n_S moderately influenced the relative effect sizes of predictors on the A-sensitivities (Figs. S9-S13). For $\mathcal{S}[\mathcal{P}_\alpha]$, as foodweb complexity (C and n_S) increased, the relative importance of T and λ increased

respect to that of $\hat{a}$. This is consistent with our first local stability analysis (Fig. S2), which showed that more complex communities display a smaller stability region on the λ-T plane. Similarly, effects of λ and T on $\mathcal{S}[\mathcal{P}_\gamma]$ increased, relative to the ones of $\hat{a}$, as foodwebs were more complex. Nonlinear predictors $T \times \hat{a}$ and $\lambda \times \hat{a}$ also exhibited stronger effects for complex foodwebs. For $\mathcal{S}[\mathcal{P}_\beta]$, increasing the foodweb complexity led to larger effect sizes of the main predictor variables, and those of $T \times \hat{a}$ and $\lambda \times \hat{a}$. The A-sensitivities $\mathcal{S}[\mathcal{B}_\beta]$ and $\mathcal{S}[\mathcal{B}_\gamma]$ showed minor changes over the foodweb complexity gradient.

DISCUSSION

Our main results show that increasing asynchrony A among site availability periods reduces both local species persistence and biomass, while it rises among-habitat dissimilarity with respect to these metrics. Interestingly, regional persistence increased with A, particularly at high dispersal rates, even though regional biomass decreased. The sensitivity of metacommunities to increased landscape asynchrony was determined by both LSFs and RSFs. Roughly speaking, dispersal was the dominant predictor of A-sensitivities across a wide array of conditions, although the contribution of LSFs (both through their main effects and interactions) had a considerable influence on the A-sensitivity of regional persistence, and among-site dissimilarity in species richness. The importance of LSFs was particularly strong for scattered/spread landscapes and complex foodwebs. Among the previous studies addressing the role of local versus RSFs on metacommunity stability, Gravel et al. (2016) and Mougi and Kondoh (2016) stand out. Gravel et al. (2016) analyze the local asymptotic stability of metacommunities, and show that the probability of a metacommunity being stable increases with the propensity to stability of local communities (governed by species richness, foodweb connectance, mean interaction strength, and self-regulation strength), as well as with dispersal rate. At the same time, they showed

that the likelihood of metacommunity stability increases with habitat complexity (number of functionally distinct sites).

Applying a similar approach, Mougi and Kondoh (2016) found that the key determinants of local community stability, namely species richness and food web connectance, also play a crucial role in shaping the stability of the entire metacommunity. In essence, more stable local communities tend to contribute to the stability of the metacommunity. Moreover, dispersal can stabilize metacommunities composed of unstable prone (i.e. more complex) communities, potentially reversing the negative complexity-stability relation under certain conditions. Our findings are in line with Gravel et al. (2016) and Mougi and Kondoh (2016) in that both local community stability and dispersal rates raise both local and regional diversity. Note that both of the mentioned studies rely on Lyapunov stability analysis. However, stronger Lyapunov stability does not necessarily guarantee system robustness in the face of dynamic habitat availability, which constitutes a structural perturbation and is the primary focus of our study. In the following paragraphs we delve into the mechanisms explaining the responses of metacommunities to asynchrony A in habitat availability and how foodweb and landscape complexity modulate these responses.

We begin by noting that increasing A tends to reduce the average temporal overlap among active sites. This inhibits dispersal, leading to lower local diversity and a larger among-site dissimilarity in species composition. However, landscape asynchrony can have positive effects on regional diversity due to a compensatory effect. This is because a larger A results in a larger fraction of the year when active sites host species, promoting the prompt colonization of newly activated sites. However, LSFs determine whether A has a net positive or negative effect on regional biodiversity, as we will elaborate on later.

Dispersal effects: The increase in $\mathcal{S}[\mathcal{P}_\alpha]$ with dispersal ability, $\hat{a}$, can be explained by examining Fig. S14. Note that the range of $\mathcal{P}_\alpha$ is smaller for smaller values of $\hat{a}$, due to dispersal limitation. Thus, small $\hat{a}$ results in small $\mathcal{P}_\alpha$, which cannot be significantly reduced by increasing A. This leads to a small $\mathcal{S}[\mathcal{P}_\alpha]$. In contrast, larger $\hat{a}$ leads to higher levels of $\mathcal{P}_\alpha$ that can be decreased readily by increments in A, yielding a negative $\mathcal{S}[\mathcal{P}_\alpha]$. These cases explain the negative effects of $\hat{a}$ on $\mathcal{S}[\mathcal{P}_\alpha]$ in Fig. 3 a, d, and g.

For dense landscapes and slow dispersal, $\mathcal{P}_\gamma$ decreased only slightly with A because having a few species-rich communities yields a high $\mathcal{P}_\gamma$. Intermediate values of $\hat{a}$ prevent reductions in $\mathcal{P}_\gamma$. For high values of $\hat{a}$, A increases $\mathcal{P}_\gamma$ in many cases, particularly for metacommunities exhibiting high $\mathcal{P}_\gamma$ when $A = 0$. This can be explained by the compensatory effect described earlier. These cases elucidate the effects of $\hat{a}$ on $\mathcal{S}[\mathcal{P}_\gamma]$ as shown in Figs. 3 c, and f. A similar response has been observed in models of competitive metacommunities and, more recently, in multitrophic metacommunities (Firkowski et al., 2022), where a positive relationship exists between spatially uncorrelated environmental fluctuations and stability. In the cases of scattered/spread landscapes, the effect of $\hat{a}$ on $\mathcal{S}[\mathcal{P}_\gamma]$ was markedly nonlinear. At low $\hat{a}$, $\mathcal{S}[\mathcal{P}_\gamma] \approx 0$ since, regardless of A, $\mathcal{P}_\gamma \approx 0$ due to dispersal limitation. Increasing $\hat{a}$ alleviates dispersal limitation, rising $\mathcal{P}_\gamma$ at $A = 0$. A higher A pushes down $\mathcal{P}_\gamma$, resulting in a negative $\mathcal{S}[\mathcal{P}_\gamma]$. At high $\hat{a}$, $\mathcal{P}_\gamma$ keeps at relatively high levels, and there is a positive $\mathcal{S}[\mathcal{P}_\gamma]$ because of the compensatory effect. The change in the sign of $\mathcal{S}[\mathcal{P}_\gamma]$ leads to the nonlinear effect of $\hat{a}$ in Fig. 3i.

Dispersal affects $\mathcal{S}[\mathcal{P}_\beta]$ nonlinearly for dense landscapes. (Figs. 3b, e), reaching a maximum and then slightly decreasing. For both small and large values of $\hat{a}$, $\mathcal{S}[\mathcal{P}_\beta]$ is small. In the first case, most sites are unpopulated and, therefore homogeneous regardless of A. In the second case, sites reachable from the mainland are homogeneously populated because of fast dispersal. Increasing A reduces the number of available sites and therefore $\mathcal{P}_\beta$ increases moderately. In contrast, for intermediate values of $\hat{a}$, both

mechanisms that raise $\mathcal{P}_\beta$ come into play. Moderate dispersal induces dissimilarity in species composition across space. Besides, landscape asynchrony reduces the number of available sites, leading to an even greater increase in $\mathcal{P}_\beta$. This yields a marked positive $\mathcal{S}[\mathcal{P}_\beta]$. The described effects of $\hat{a}$ on $\mathcal{S}[\mathcal{P}_\beta]$, along with the underlying mechanisms, also apply to scattered/spread landscapes. Here, landscape asynchrony increases $\mathcal{P}_\beta$ at high $\hat{a}$. The increased average distance among sites in scattered/spread landscapes lowers effective rates of dispersal, potentially weakening its homogenizing effect.

The patterns of metacommunity A-sensitivity of biomass can be explained using similar arguments as those stated before. Basically, dispersal ability fosters biomass abundance, and homogenization across sites. Therefore, $\hat{a}$ has a positive effect on $\mathcal{S}[\mathcal{B}_\beta]$ and a negative effect on $\mathcal{S}[\mathcal{B}_\gamma]$ (see Fig. 2 and S7-S8 and S12-S13).

Our results align with earlier studies that emphasize the critical role of dispersal as a driving force behind metacommunity dynamics and resultant diversity patterns. The influential work of Mouquet and Loreau (2002, 2003), assuming a spatially implicit patch dynamics archetype for competitive metacommunities, posited that dispersal leads to a humped response in α-diversity, accompanied by decreasing trends in both β-diversity and γ-diversity. Recently, Thompson et al. (2020) uadopted a more comprehensive approach encompassing a wider range of archetypes and identified similar trends to those in Mouquet and Loreau (2002, 2003), albeit with qualitative differences for some settings. Presently, research examining the impacts of dispersal on multitrophic metacommunities (e.g. Ye and Wang (2023)) yields results analogous to those observed in competitive metacommunities.

However, these theoretical predictions often diverge from empirical results (Grainger and Gilbert, 2016). In our metacommunity assembly model, we obtained positive responses of $\mathcal{P}_\alpha$ and $\mathcal{P}_\gamma$, and a negative response of $\mathcal{P}_\beta$ to increases in a. When considering landscapes subjected to perturbations, dispersal can mitigate their impact on local populations by subsidizing populations from undisturbed sites (Altermatt et al., 2011a). However,

in multitrophic metacommunities, the ability of dispersal to maintain local populations differs among trophic groups (Limberger et al., 2019; Ryser et al., 2021). In our study, we found that dispersal: a) magnifies the negative effect of A on $\mathcal{P}_\alpha$. b) magnifies the positive effect of A on $\mathcal{P}_\beta$ over a large region of the parameter space. c) shifts the effect of A on $\mathcal{P}_\gamma$ from negative to positive.

Effects of local stabilizing factors: Explaining why LSFs (predictors T and λ) have a significant effect on metacommunity sensitivity, especially on $\mathcal{S}[\mathcal{P}_\gamma]$, is straightforward when examining Figs. S14-S15. Note that for large values of a, regardless of A and n_P, stable-prone foodwebs tend to produce metacommunities with high regional persistences. We observe a similar trend for $\mathcal{S}[\mathcal{P}_\alpha]$ at $A = 0$. We illustrate the processes behind these trends by analyzing metacommunity dynamics on idealized star-shaped landscapes (see Appendix S1, Section Star experiment).

This experiment reveals that all effects of LSFs on A-sensitivities can be explained by the interplay among the time-averaged values of three variables: the number of available sites, the number of species per site, and the dissimilarity of species composition among sites. Regardless of local stability-proneness, a reduction in available sites by increasing A drives down $\mathcal{P}_\alpha$. While for stable-prone foodwebs all available sites hosted essentially all species, for unstable-prone foodwebs, available sites hosted a small fraction of the species pool, which leads to a decrease in $\mathcal{P}_\alpha$. In contrast to stable-prone foodwebs, unstable-prone foodwebs induce a high among-site heterogeneity in species composition. This, combined with the reduction in available sites, results in a decrease in $\mathcal{P}_\gamma$. This yields relatively high $\mathcal{P}_\gamma$ values in spite of the low $\mathcal{P}_\alpha$.

From previous considerations, for unstable-prone communities, $\mathcal{P}_\alpha$ maintains low values regardless of A resulting in a small $\mathcal{S}[\mathcal{P}_\alpha]$. For stable-prone communities, $\mathcal{P}_\alpha$ is high for $A = 0$ and low for high A values. Thus, $\mathcal{S}[\mathcal{P}_\alpha]$ becomes very negative. Hence $\mathcal{S}[\mathcal{P}_\alpha]$ decreases with local stability-proneness. Similarly, for unstable-prone communities $\mathcal{P}_\gamma$

decreases as A increases, resulting in a negative $\mathcal{S}[\mathcal{P}_\gamma]$. For stable-prone communities, $\mathcal{P}_\gamma$ remains insensitive to changes in A. Therefore, $\mathcal{S}[\mathcal{P}_\gamma]$ increases with local stability-proneness. The combination of few species per site and limited available sites leads to a very small $\mathcal{P}_\alpha$ for unstable-prone communities and high values of A. Also, $\mathcal{P}_\gamma$ is relatively high, resulting in a large $\mathcal{P}_\beta$. This explains the negative effects of local stability-proneness on $\mathcal{S}[\mathcal{P}_\beta]$. In the case of scattered landscapes, the effects of T and λ on $\mathcal{S}[\mathcal{P}_\beta]$ were negligible. This is due to the longer routes for dispersal (i.e. longer distances between adjacent sites), which makes dispersal rate outweigh all the other predictors.

Spatial heterogeneity in community biomass is also altered by LSFs. Specifically, $\mathcal{B}_\gamma$ decreases with A, although local stability proneness buffers this reduction in metacommunity biomass. LSFs do not exert any noticeable effect on $\mathcal{S}[\mathcal{B}_\beta]$.

Effects of landscape structure: There has been a growing acknowledgment of the importance of landscape structure on metacommunity diversity (Economo and Keitt, 2008; Galiana et al., 2018; Borthagaray et al., 2023b,a). Moreover, environmental changes alter landscape structure at different temporal and spatial scales (Holyoak et al., 2020). Earlier spatially implicit metapopulation models show that species persistence is highly sensitive to landscape dynamics (Keymer et al., 2000; Reigada et al., 2015). In a metacommunity context, using an experimental system of only two sites, Altermatt et al. (2011a) showed that local population densities and species persistence exhibit different responses to periodic perturbations on local sites and that dispersal capabilities play a key role in the recovery of species after perturbations. To understand and project the consequences of these changes on biodiversity it is natural to resort to an approach based on spatially explicit, dynamic landscapes. More recent advances using a neutral spatially explicit model, highlight that temporal changes in landscape structure may shape metacommunity biodiversity, showing that fluctuating landscape connectivity may enhance local and regional diversity, relative to static landscapes with constant connectivity (Marco Palamara et al., 2023). In

this study, we explore the behavior of multitrophic metacommunities in spatially explicit dynamic landscapes.

The most notorious effects of landscape structure is related to the number of sites and its influence on β and γ diversity, and metacommunity biomass. Landscapes with more sites imply shorter distances between sites, resultig in faster dispersal. This leads to a positive effect of n_P on $\mathcal{P}_\gamma$. A similar effect is observed for F on $\mathcal{P}_\gamma$ because of the short distances between the mainland and each site in its module. Regardless of landscape structure, asynchrony reduces the availability of dispersal routes among sites by drastically reducing (or even canceling) the time intervals during which dispersal between sites is possible. The effect of a on $\mathcal{S}[\mathcal{P}_\gamma]$ is stronger on denser and more modular landscapes. This is due to the combination of the positive effect of a, described earlier, the positive effects of n_P and F on dispersal rates, and n_P increasing the probability of having (asynchronously) activated sites present throughout the season. The relationship between n_P and F and dispersal rates also helps explain the observed patterns of variation of $\mathcal{S}[\mathcal{P}_\beta]$ across landscape structure parameters. The number of sites n_P strengthens the effect of a on $\mathcal{S}[\mathcal{B}_\gamma]$ because regardless of A, when a is very small, $\mathcal{B}_\gamma \approx 0$ due to dispersal limitations, and $\mathcal{S}[\mathcal{B}_\gamma] \approx 0$. For large values of a, and $A = 0$, we have optimal dispersal conditions, and metacommunity biomass is proportional to n_P. Also, $\mathcal{B}_\gamma(A = 1/2) \ll \mathcal{B}_\gamma(A = 0)$ because of a low site occupancy for highly asynchronous landscape dynamics, regardless of n_P. It follows that the effect size of a grows with n_P. Then, the negative effect of landscape asynchrony on metacommunity biomass rises with a and n_P.

It follows that the effect size of a increases with n_P, and consequently, the negative impact of landscape asynchrony on metacommunity biomass is amplified with higher values of both a and n_P."

The effect of LSFs on A-sensitivities increases with both landscape density and modularity. In denser and more modular landscapes, there are many sites near the mainland. In this

scenario $\mathcal{P}_\gamma$ decreases with asynchrony among sites hosting unstable-prone communities, due to a lower colonization success that leads to fewer species-rich sites. Conversely, with stable-prone communities, colonization is more successful, leading to a higher fraction of rich communities near the mainland. This process, added to the temporal aggregation effect, increases $\mathcal{P}_\gamma$ with higher landscape asynchrony. However, these processes do not occur in scattered/spread landscapes, where longer site-mainland distances strongly limit dispersal and prevent increasing $\mathcal{P}_\gamma$. The same mechanisms also contribute to explaining the variation in $\mathcal{B}_\gamma$ with different landscape structures.

Effects of foodweb structure: Unlike Gravel et al. (2011), we did not find clear evidence of a positive relation between foodweb complexity and regional species persistence. This is not surprising, given the several differences between our model (explicit landscape with nonrandom structure, equilibrium dynamics of species) and theirs (implicit and fully connected landscape, patch dynamics). This issue deserves further study. Our results indicate that the more complex foodwebs are, the larger the effects of LSFs on A-sensitivities of $\mathcal{P}_\alpha$, $\mathcal{P}_\beta$, and $\mathcal{P}_\gamma$. The negative effects of n_S, and C on local community stability proneness are similar to those of T and $-\lambda$. The high importance of LSFs exhibited by complex foodwebs can be explained by the high values of P_β reached when communities are unstable-prone. The operating mechanism behind the positive effects of LSFs on $\mathcal{S}[\mathcal{P}_\gamma]$ was explained using the star experiment (see Appendix S1 Section Star experiment). This effect vanishes for inherently stable foodwebs, such as those with low n_S and C, because LSFs are less critical in determining equilibrium population sizes, extinction probability, and receptivity to immigrants. Using similar arguments we can explain why the effect sizes of LSFs on $\mathcal{S}[\mathcal{P}_\alpha]$ and $\mathcal{S}[\mathcal{P}_\beta]$ increase with the foodweb complexity.

Final remarks: Our model is based on a random matrix approach (May, 1972; Allesina and Tang, 2012) for local communities connected by stochastic dispersal over an explicit random dynamic landscape. This modeling strategy differs from the more frequently used approaches for representing multitrophic metacommunities, as reviewed in Gross et al. (2020). Avoiding numerical integration by focusing on species equilibria, as opposed to transient behavior, allows us to simulate multitrophic metacommunities with many species and many sites efficiently. Our use of a continuous-time Markov chain provides a straightforward means of representing migration events and simulating landscape dynamics with stochastic asynchrony. Finally, our model allows for the coupling of site (de)activation and migration events with changes in local species biomasses via recalculating equilibria at the arrival sites. For future research, our model can be easily extended to incorporate other relevant processes. For instance, it would be worth to introduce heterogeneity in site quality (Thompson and Gonzalez, 2017; Ryser et al., 2021; Ye and Wang, 2023), and dispersal gradients governed by physical (Altermatt et al., 2011b) or ecological Reigada et al. (2015) conditions.

Previous studies (May, 1972; Allesina and Tang, 2012) provided valuable insights into isolated community responses to small acute perturbations of species' abundances by analyzing the Lyapunov stability of linearized systems. However, the role of local stability in a metacommunity context is still not well understood, especially in fluctuating environments. Here, we integrate the roles of local community stability and of connectivity among communities driven by dispersal, in shaping the responses of trophic metacommunities to quasiperiodic habitat creation and destruction. We also present mechanisms that explain how landscape and foodweb complexity determine the relative importance of local versus regional stabilizing factors in maintaining biodiversity patterns in dynamic landscapes. Our findings hold particular relevance in light of the high and growing prevalence of temporary ecosystems, especially aquatic ones (Smol and Douglas, 2007;

Fernandes et al., 2014; Datry et al., 2016; Parra et al., 2021). Human activities, both directly and indirectly, alter the dynamics of temporary systems, potentially causing adverse consequences for biodiversity. Our contributions add to the theory of trophic metacommunities and the field of ecological networks on dynamic landscapes (Zeigler and Fagan, 2014; Holyoak et al., 2020; Fortin et al., 2021), which require further development in view of the current environmental concerns. As a promising avenue for future research, we envision expanding our model to delve into the complex interactions between landscape dynamics and the evolutionary and behavioral adaptations to shifts in abiotic conditions and biotic interactions.

ACKNOWLEDGMENTS

This study was supported by grant ANID/FONDECYT 1231321.

References

Aiken, C. M. and Navarrete, S. A. (2014). Coexistence of competitors in marine metacommunities: environmental variability, edge effects, and the dispersal niche. *Ecology*, 95(8):2289–2302.

Allesina, S. and Tang, S. (2012). Stability criteria for complex ecosystems. *Nature*, 483(7388):205–208.

Altermatt, F., Bieger, A., Carrara, F., Rinaldo, A., and Holyoak, M. (2011a). Effects of connectivity and recurrent local disturbances on community structure and population density in experimental metacommunities. *PloS one*, 6(4):e19525.

Altermatt, F., Schreiber, S., and Holyoak, M. (2011b). Interactive effects of disturbance and dispersal directionality on species richness and composition in metacommunities. *Ecology*, 92(4):859–870.

Arancibia, P. A. and Morin, P. J. (2022). Network topology and patch connectivity affect dynamics in experimental and model metapopulations. *Journal of Animal Ecology*, 91(2):496–505.

Barabás, G., Michalska-Smith, M. J., and Allesina, S. (2017). Self-regulation and the stability of large ecological networks. *Nature ecology & evolution*, 1(12):1870–1875.

Borthagaray, A. I., Barreneche, J. M., Abades, S., and Arim, M. (2014). Modularity along organism dispersal gradients challenges a prevailing view of abrupt transitions in animal landscape perception. *Ecography*, 37(6):564–571.

Borthagaray, A. I., Cunillera-Montcusí, D., Bou, J., Biggs, J., and Arim, M. (2023a). Pondscape or waterscape? the effect on the diversity of dispersal along different freshwater ecosystems. *Hydrobiologia*, pages 1–13.

Borthagaray, A. I., Cunillera-Montcusí, D., Bou, J., Tornero, I., Boix, D., Anton-Pardo, M., Ortiz, E., Mehner, T., Quintana, X. D., Gascón, S., et al. (2023b). Heterogeneity in the isolation of patches may be essential for the action of metacommunity mechanisms. *Frontiers in Ecology and Evolution*, 11:1125607.

Borthagaray, A. I., Soutullo, A., Carranza, A., and Arim, M. (2018). A modularity-based approach for identifying biodiversity management units. *Revista chilena de historia natural*, 91(1):1–10.

Brendonck, L., Pinceel, T., and Ortells, R. (2017). Dormancy and dispersal as mediators of zooplankton population and community dynamics along a hydrological disturbance gradient in inland temporary pools. *Hydrobiologia*, 796(1):201–222.

Chesson, P. (2000). Mechanisms of maintenance of species diversity. *Annual review of Ecology and Systematics*, pages 343–366.

Chesson, P. and Huntly, N. (1989). Short-term instabilities and long-term community dynamics. *Trends in Ecology & Evolution*, 4(10):293–298.

Datry, T., Bonada, N., and Heino, J. (2016). Towards understanding the organisation of metacommunities in highly dynamic ecological systems. *Oikos*, 125(2):149–159.

Economo, E. P. and Keitt, T. H. (2008). Species diversity in neutral metacommunities: a network approach. *Ecology letters*, 11(1):52–62.

Economo, E. P. and Keitt, T. H. (2010). Network isolation and local diversity in neutral metacommunities. *Oikos*, 119(8):1355–1363.

Erős, T., Sály, P., Takács, P., Specziár, A., and Bíró, P. (2012). Temporal variability in the spatial and environmental determinants of functional metacommunity organization–stream fish in a human-modified landscape. *Freshwater Biology*, 57(9):1914–1928.

Fernandes, I. M., Henriques-Silva, R., Penha, J., Zuanon, J., and Peres-Neto, P. R. (2014). Spatiotemporal dynamics in a seasonal metacommunity structure is predictable: the case of floodplain-fish communities. *Ecography*, 37(5):464–475.

Firkowski, C. R., Thompson, P. L., Gonzalez, A., Cadotte, M. W., and Fortin, M.-J. (2022). Multi-trophic metacommunity interactions mediate asynchrony and stability in fluctuating environments. *Ecological Monographs*, 92(1):e01484.

Fortin, M.-J., Dale, M. R., and Brimacombe, C. (2021). Network ecology in dynamic landscapes. *Proceedings of the Royal Society B*, 288(1949):20201889.

Galiana, N., Lurgi, M., Claramunt-López, B., Fortin, M.-J., Leroux, S., Cazelles, K., Gravel, D., and Montoya, J. M. (2018). The spatial scaling of species interaction networks. *Nature Ecology & Evolution*, 2(5):782–790.

Gillespie, D. T. (1976). A general method for numerically simulating the stochastic time evolution of coupled chemical reactions. *Journal of computational physics*, 22(4):403–434.

Grainger, T. N. and Gilbert, B. (2016). Dispersal and diversity in experimental metacommunities: linking theory and practice. *Oikos*, 125(9):1213–1223.

Gravel, D., Canard, E., Guichard, F., and Mouquet, N. (2011). Persistence increases with diversity and connectance in trophic metacommunities. *PloS one*, 6(5):e19374.

Gravel, D., Massol, F., and Leibold, M. A. (2016). Stability and complexity in model meta-ecosystems. *Nature communications*, 7(1):12457.

Gross, T., Allhoff, K. T., Blasius, B., Brose, U., Drossel, B., Fahimipour, A. K., Guill, C., Yeakel, J. D., and Zeng, F. (2020). Modern models of trophic meta-communities. *Philosophical Transactions of the Royal Society B*, 375(1814):20190455.

Harary, F. and Gupta, G. (1997). Dynamic graph models. *Mathematical and Computer Modelling*, 25(7):79–87.

Holyoak, M. (2000). Habitat patch arrangement and metapopulation persistence of predators and prey. *The American Naturalist*, 156(4):378–389.

Holyoak, M., Caspi, T., and Redosh, L. W. (2020). Integrating disturbance, seasonality, multi-year temporal dynamics, and dormancy into the dynamics and conservation of metacommunities. *Frontiers in Ecology and Evolution*, 8:571130.

Hooper, D. U., Adair, E. C., Cardinale, B. J., Byrnes, J. E., Hungate, B. A., Matulich, K. L., Gonzalez, A., Duffy, J. E., Gamfeldt, L., and O'Connor, M. I. (2012). A global synthesis reveals biodiversity loss as a major driver of ecosystem change. *Nature*, 486(7401):105–108.

Hui, C., Richardson, D. M., Landi, P., Minoarivelo, H. O., Garnas, J., and Roy, H. E. (2016). Defining invasiveness and invasibility in ecological networks. *Biological Invasions*, 18(4):971–983.

Johnson, S., Domínguez-García, V., Donetti, L., and Munoz, M. A. (2014). Trophic coherence determines food-web stability. *Proceedings of the National Academy of Sciences*, 111(50):17923–17928.

Jost, L. (2007). Partitioning diversity into independent alpha and beta components. *Ecology*, 88(10):2427–2439.

Kéfi, S., Domínguez-García, V., Donohue, I., Fontaine, C., Thébault, E., and Dakos, V. (2019). Advancing our understanding of ecological stability. *Ecology Letters*, 22(9):1349–1356.

Keymer, J. E., Marquet, P. A., Velasco-Hernández, J. X., and Levin, S. A. (2000).

Extinction thresholds and metapopulation persistence in dynamic landscapes. *The American Naturalist*, 156(5):478–494.

Klaise, J. and Johnson, S. (2016). From neurons to epidemics: How trophic coherence affects spreading processes. *Chaos: An Interdisciplinary Journal of Nonlinear Science*, 26(6):065310.

Leibold, M. A., Holyoak, M., Mouquet, N., Amarasekare, P., Chase, J. M., Hoopes, M. F., Holt, R. D., Shurin, J. B., Law, R., Tilman, D., et al. (2004). The metacommunity concept: a framework for multi-scale community ecology. *Ecology letters*, 7(7):601–613.

Limberger, R., Pitt, A., Hahn, M. W., and Wickham, S. A. (2019). Spatial insurance in multi-trophic metacommunities. *Ecology Letters*, 22(11):1828–1837.

Loreau, M. and De Mazancourt, C. (2013). Biodiversity and ecosystem stability: a synthesis of underlying mechanisms. *Ecology letters*, 16:106–115.

Lurgi, M., Galiana, N., López, B. C., Joppa, L. N., and Montoya, J. M. (2014). Network complexity and species traits mediate the effects of biological invasions on dynamic food webs. *Frontiers in Ecology and Evolution*, 2:36.

Marco Palamara, G., Rozenfeld, A., de Santana, C. N., Klecka, J., Riera, R., Eguíluz, V. M., and Melián, C. J. (2023). Biodiversity dynamics in landscapes with fluctuating connectivity. *Ecography*, page e06385.

May, R. M. (1972). Will a large complex system be stable? *Nature*, 238(5364):413–414.

McCann, K. S. (2000). The diversity–stability debate. *Nature*, 405(6783):228–233.

Mougi, A. and Kondoh, M. (2016). Food-web complexity, meta-community complexity and community stability. *Scientific reports*, 6(1):1–5.

Mouquet, N. and Loreau, M. (2002). Coexistence in metacommunities: the regional similarity hypothesis. *The American Naturalist*, 159(4):420–426.

Mouquet, N. and Loreau, M. (2003). Community patterns in source-sink metacommunities. *The american naturalist*, 162(5):544–557.

Olmo, C., Gálvez, Á., Bisquert-Ribes, M., Bonilla, F., Vega, C., Castillo-Escrivà, A., De Manuel, B., Rueda, J., Sasa, M., Ramos-Jiliberto, R., et al. (2022). The environmental framework of temporary ponds: A tropical-mediterranean comparison. *Catena*, 210:105845.

Parra, G., Guerrero, F., Armengol, J., Brendonck, L., Brucet, S., Finlayson, C. M., Gomes-Barbosa, L., Grillas, P., Jeppesen, E., Ortega, F., et al. (2021). The future of temporary wetlands in drylands under global change. *Inland Waters*, 11(4):445–456.

Reigada, C., Schreiber, S. J., Altermatt, F., and Holyoak, M. (2015). Metapopulation dynamics on ephemeral patches. *The American Naturalist*, 185(2):183–195.

Rohr, R. P., Saavedra, S., and Bascompte, J. (2014). On the structural stability of mutualistic systems. *Science*, 345(6195):1253497.

Ryser, R., Hirt, M. R., Häussler, J., Gravel, D., and Brose, U. (2021). Landscape heterogeneity buffers biodiversity of simulated meta-food-webs under global change through rescue and drainage effects. *Nature Communications*, 12(1):4716.

Smol, J. P. and Douglas, M. S. (2007). Crossing the final ecological threshold in high arctic ponds. *Proceedings of the national Academy of Sciences*, 104(30):12395–12397.

Suzuki, Y. and Economo, E. P. (2021). From species sorting to mass effects: spatial network structure mediates the shift between metacommunity archetypes. *Ecography*, 44(5):715–726.

Thébault, E. and Fontaine, C. (2010). Stability of ecological communities and the architecture of mutualistic and trophic networks. *Science*, 329(5993):853–856.

Thompson, P. L. and Gonzalez, A. (2017). Dispersal governs the reorganization of ecological networks under environmental change. *Nature Ecology & Evolution*, 1(6):1–8.

Thompson, P. L., Guzman, L. M., De Meester, L., Horváth, Z., Ptacnik, R., Vanschoenwinkel, B., Viana, D. S., and Chase, J. M. (2020). A process-based metacommunity framework linking local and regional scale community ecology. *Ecology letters*, 23(9):1314–1329.

Wilcox, K. R., Tredennick, A. T., Koerner, S. E., Grman, E., Hallett, L. M., Avolio, M. L., La Pierre, K. J., Houseman, G. R., Isbell, F., Johnson, D. S., et al. (2017). Asynchrony among local communities stabilises ecosystem function of metacommunities. *Ecology letters*, 20(12):1534–1545.

Ye, X. and Wang, S. (2023). Maintenance of biodiversity in multitrophic metacommunities: Dispersal mode matters. *Journal of Animal Ecology*.

Zeigler, S. L. and Fagan, W. F. (2014). Transient windows for connectivity in a changing world. *Movement Ecology*, 2(1):1–10.

Figure 1 Species persistence (A) and $\log_{10}$ community biomass (B), in a single local community with colonization from a regional pool, as a function of foodweb diagonal values ($-\lambda$) and foodweb temperature values T. Foodweb complexity parameters are $n_S = 45$ and $C = 0.2$. Each cell value shows the mean of 50 replicates.

Figure 2 Relative change of each response variable when changing landscape asynchrony A from 0.0 to 0.5 at two values of dispersal ability a. Mean and SE over 50 replicates, with $n_S = 45$, $C = 0.2$, $n_P = 100$, $F = 50$, $T = 0.2$, and $\lambda = 0.47$

Figure 3 Effect sizes on A-sensitivities $\mathcal{S}[\mathcal{P}_\alpha]$, $\mathcal{S}[\mathcal{P}_\beta]$, and $\mathcal{S}[\mathcal{P}_\gamma]$. Predictors are foodweb temperature T (1), self limitation λ (2), dispersal ability $\hat{a} = \log_{10} a$ (3), $T \cdot \lambda$ (4), $T \times \hat{a}$ (5), $\lambda \times \hat{a}$ (6), T^2 (7), λ^2 (8), and $\hat{a}^2$ (9). Parameters are $n_S = 45$, $C = 0.2$, $n_P = 50$, $F = 50$ (base parameters, a-c); $n_S = 75$, $C = 0.25$, $n_P = 50$, $F = 50$ (complex foodwebs, d-f); $n_S = 45$, $C = 0.2$, $n_P = 10$, $F = 5$ (scattered/spread landscapes, g-i)

Figure 1

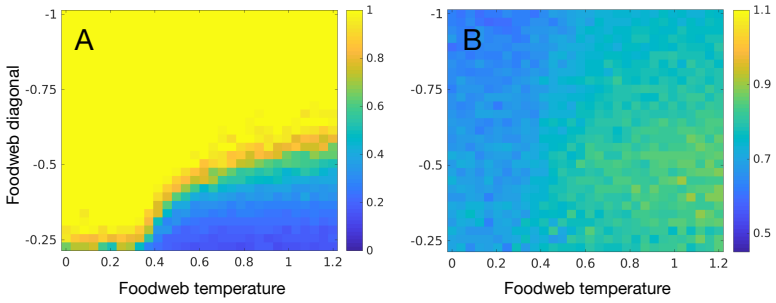

Fig. 1

Figure 2

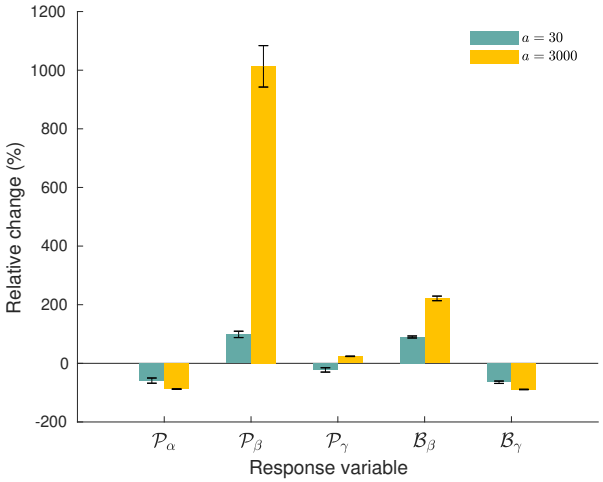

Fig. 2

Figure 3

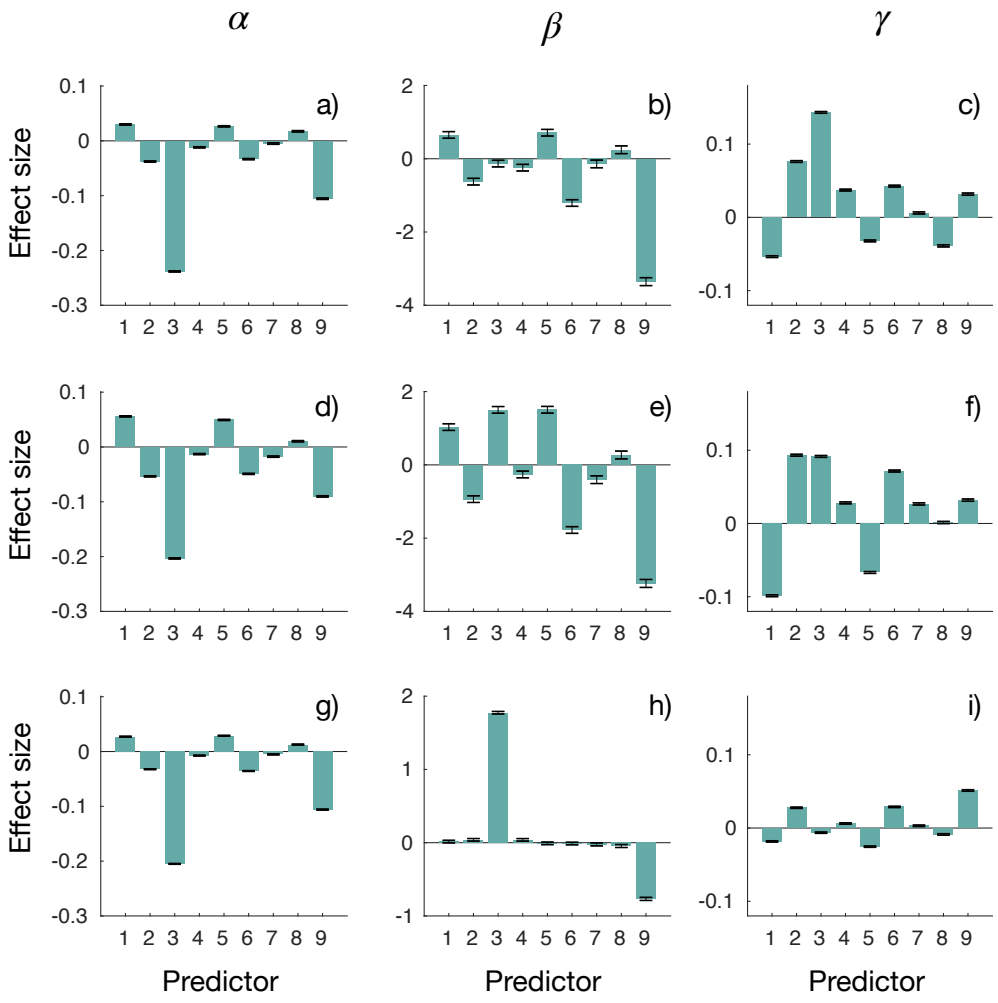

Fig. 3

APPENDIX S1 *DETAILED METHODS AND ADDITIONAL RESULTS*

S1.1 Detailed methods

Landscape generation and dynamics: We represent dynamic landscapes as dynamic graphs, i.e. time-varying graphs with node-dynamics (Harary and Gupta, 1997). Vertices represent sites where local communities can be assembled, edges represent a non-zero probability of species dispersal between sites, and edge weights represent the Euclidean distance between two adjacent sites. Our algorithm creates connected modular landscapes by laying sites at random on a square, creating a minimum spanning tree, and then adding edges at random to reach a desired connectance. The process uses five parameters, namely n_P, n_E, n_C, F, and x. They represent the number of sites, the number of edges, the number of modules, the excess factor, and the distance exponent. The first three are self-explanatory. We fixed n_E to $2n_P$ and n_C to 5. Real parameter $F \geq 1$ regulates how tight the modules are. A value of 1 results in no discernible clustering of sites, i.e. they are distributed uniformly at random, while a high value will produce tight modules. Real parameter $x \geq 0$ controls how the distances among sites determine the probability of edges being added to the landscape. A value of zero indicates that distances between sites do not affect the probability of edges being added. A larger value favors adding shorter edges over longer ones. Thus, spatial modularity increases with both F and x. See Figure S1 for an example. We set $x = 2$ for all our simulations. A site of a randomly chosen module is designated as *the mainland*.

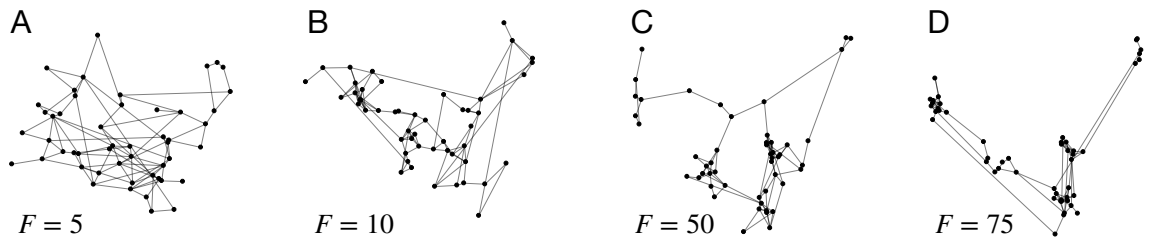

Fig. S1. Examples of landscapes with different degrees of spatial modularity generated by our algorithm through varying excess factor F. We used 50 sites, 100 edges, 5 modules, and a distance exponent of 2.

At a given time, each site p is in either of two states: "active" or "inactive." Species can be present in p only when the site is "active." The mainland is always "active", and all species in the regional pool are present therein. All the other sites transition stochastically between the two states. For a site p, the nominal length of the "active" period is randomly drawn from a uniform distribution $w_p \sim U(0.2, 0.3)$. Assuming no overlapping "active" periods from consecutive years, the start of the "active" period for the year k is $start_{p,k} = k + z_{p,k}$, where $z_{p,k} \sim U(-A, +A)$, and parameter $A > 0$ is the magnitude of asynchrony among the sites' activation times. The end of the period will be $end_{p,k} = start_{p,k} + w_p$. To account for overlaps, we define $ACTIVE_p = \cup_k [start_{p,k}, end_{p,k}]$ and we say site p is "active" at time t if and only if $t \in ACTIVE_p$.

Modular landscape generation algorithm

```
function modular_landscape(n_P, n_E, F, n_C, x)
   // Choose potential locations for sites.
   // Locations are points on the real (x,y) plane.
   Let L be an array of ⌊n_S · F⌋ points in a 512 × 512 square randomly drawn
      from a uniform distribution.

   // Select the first n_C of these locations as cluster centers
   Let C = {1, 2, ..., n_C}.
```

// Compute all pairwise distances, and the distances to the closest center
Let $d_{i,j}$ be the euclidean distance between points L_i and L_j
Let $\delta_i = \min_{j \in C} d(i,j)$

// Randomly select the non–center sites and combine with centers, yielding
// the final set of sites S.
Let V be a set of $n_S - n_C$ integers from $\{n_C + 1, n_C + 2, \ldots, \lfloor n_S \cdot F \rfloor\}$ chosen with probabilities inversely proportional to δ_i
Let $P = C \cup V$ // These vertices will be the landscape sites

// Compute a minimum spanning tree of the clique of all final sites
Let $K = (P, P \times P)$ // A complete graph with all the vertices
Let $Tree = MST(K)$ using distances $d_{i,j}$
Let $E_T = edges(Tree)$

// Randomly choose the remaining edges
Let E be a set of $n_E - n_P + 1$, randomly chosen undirected edges from $P \times P - E_T$
The probability to choose (i,j) is inversely proportional to $d_{i,j}^x$

Return $G = (P, E + E_T)$ and the weights $d_{i,j}$ for all the edges in G
end

Local community dynamics: The regional pool of species and interactions is modeled as a foodweb following Klaise and Johnson (2016), which extends the Preferential Prey Model (Johnson et al., 2014). Unlike the niche or the cascade models, the algorithm in Klaise and Johnson (2016) creates foodwebs with varying degrees of trophic coherence, a structural property that strongly determines stability in empirical and quasi-empirical foodwebs (Johnson et al., 2014). The algorithm creates foodweb topologies from target values of species richness n_S, number of basal species n_B, number of predation links n_L, and foodweb temperature T (a surrogate for trophic coherence). We fixed the number of basal species to 20% of the species richness. We define foodweb connectance C as $n_L/(n_S \cdot (n_S - n_B - 1) + n_B)$, i.e. the ratio between the number of present links n_L and the maximum possible number of edges in a foodweb with n_B basal species and no cannibals.

We assume that the dynamics of $x_{i,p}$, the biomass of species i at site p, is governed by Lotka-Volterra type equations and reaches equilibrium instantaneously. The ODEs

describing local community dynamics are:

$$\frac{dx_{i,p}}{dt} = \left(r_i + \sum_j M_{ij} x_{j,p} \right) x_{i,p}, \tag{S1}$$

where i and j range over all species in the pool. Elements $M_{i,j}$ of the *community matrix* M represent the effect of increasing population biomass of species j on the per unit biomass growth rate of species i. Parameters r_i's are the intrinsic growth rates.

To define M, we first assign $M_{ii} = -\lambda$, where the self-regulation parameter λ is a positive real. If there are no trophic interactions between species i and j, then $M_{ij} = 0$. If j feeds on i, then $M_{ij} = -\mathcal{X}$, where $\mathcal{X}$ is drawn from a lognormal distribution, with mean 1 and a standard deviation of 0.25. Following Johnson et al. (2014), we set $M_{ji} = 0.4\mathcal{X}$. To choose the values for the r_i's, we solve the linear program:

$$\begin{aligned}
&\max y^* \\
r_i^* + \sum_j M_{ij} x_j^* &= 0 \\
x_i^* &\geq y^* \\
y^* &\geq 0 \\
r_i^* &\leq \rho && \text{for basal species } i \\
r_i^* &\leq -\mu && \text{for non-basal species } i.
\end{aligned}$$

We set $\rho = 1$ to limit the intrinsic growth rate for basals. Parameter $\mu = 0.01$ is the smallest possible mortality rate value for non-basal species. The decision variables are y^*, all the r_i^*'s, and all the x_i^*'s. Maximizing y^* means maximizing the smallest species abundance at equilibrium. If the program is not feasible, then it is impossible to choose

r_i^*'s in such a way that all the x_i^*'s are positive. If this happens, the foodweb is discarded and the process is repeated. If the program is feasible, we check that, at equilibrium (the values obtained for the x_i^*'s), the Jacobian matrix of Eq. (S1) has only eigenvalues with negative real parts. If this is not the case, then the system is unstable and it is discarded to start the process again.

Metacommunity dynamics: Dispersal is modeled as a continuous time Markov chain. The dispersal events, i.e. individuals moving from one site to another one, are coupled with events representing the activation and deactivation of landscape sites, and with the local community dynamics. A dispersal event of a species s from site p to site q is only possible if sites p and q are active, s is present in p but not in q, and s is either a basal species or a consumer with at least one of its prey species present in q. The biomasses of all species present in q are recomputed as the equilibrium of Eq. S1 and set to zero for all species whose value is below an extinction threshold of 0.001. If at least one species goes extinct, equilibrium is recalculated until no further secondary extinctions occur. The set of species in p is not altered by dispersal events originating from p. The *effective rate* of dispersal events between sites p and q is the ratio between the dispersal ability $a \in \mathbb{R}^+$ and the Euclidean distance between p and q. However, if this ratio is less than 0.1, we set the rate to zero. Site deactivation drives all species' biomasses in that site to zero. To perform our simulations, we use a variant of the first-reaction method (Gillespie, 1976), in the framework of dynamic Monte Carlo methods.

Metacommunity simulation algorithm

There are three types of events:

1. Site activation events, described as triples $\langle t, p, \text{`}activate\text{'}\rangle$, meaning at time t site p becomes active.

2. Site deactivation events, described as triples $\langle t, p, \text{`deactivate'}\rangle$, meaning at time t site p becomes inactive.

3. Dispersal events, described as triples $\langle t, s, dest\rangle$, meaning at time t individuals of species s move to site *dest*.

The algorithm begins by initializing the event queue with site activation/deactivation events. Let $\mathcal{S}$ be the set of all species and let $\mathcal{P}$ be the set of all landscape sites. For every site p, define the pulse train function $f_p(t) = 1$ if $t \in ACTIVE_p$ and zero otherwise. Let $t^{on}_{p,k}$ be the rising time of the k-th pulse in f_p. Event $\langle t^{on}_{p,k}, p, \text{`activate'}\rangle$ is added to the queue. Similarly, define $t^{off}_{p,k}$ as the falling time of the $k$-th pulse in $f_p$ and add $\langle t^{off}_{p,k}, p, \text{`deactivate'}\rangle$ to the queue.

Conceptually, the algorithm to simulate the metacommunity dynamics is as follows:

```
Init queue Q with site activation/deactivation events

// Set initial state of the systems
for all sites p
   // C[p] is the set of species present at site p
   C[p] = S if p is the mainland
   C[p] = {} if p is insular
   A[p] = 'inactive' // A[p] is the state ('active' or 'inactive') of site p
end


time = 0

while Q ≠ {} //Main simulation loop
   ⟨t_m, s, dest⟩ = next_migration_event()
   ⟨t, p, type⟩ = earliest(Q)
   if t < t_m
      if type='activate'
         A[p] = 'active'
      else
         C[p] = {}
         A[p] = 'inactive'
      end
      Q = Q − ⟨t, p, type⟩
      time = t
   else
```

```
        migration_process(s, dest)
        time = t_m
    end
end

function next_migration_event()
    C1 = {⟨s, dest, orig⟩ such that
            s ∉ C[dest]
            s ∈ C[orig]
            A[dest] = 'active'
            s is basal or preys(s)∩C[dest] ≠ {}}
    C2 = {⟨τ, s, dest, orig⟩ such that
              ⟨s, dest, orig⟩ ∈ C1 and
              τ ~ exp(distance(orig, dest)/a))}
     ⟨τ, s, dest, orig⟩ = earliest(C2)
     return ⟨τ + time, s, dest⟩
end

function migration_process(s, dest)
    C[dest] = C[dest] ∪ {s}
    repeat
        solve
            r_i + Σ_j CM_ij x_j = 0 for i, j ∈ C[dest]
        C[dest] = C[dest] − {s'|x_s' < 0.001}
    until for all k ∈ C[dest], x_k ≥ 0.001
end
```

S1.2 Power mean

Let ρ be a real parameter, let t_0 and t_1 be reals and let $y(t)$ be an integrable function in (t_0, t_1). The average value of y on (t_0, t_1) is

$$\left(\frac{1}{t_1 - t_0}\int_{t_0}^{t_1} y(t)^\rho dt\right)^{\frac{1}{\rho}}. \tag{S2}$$

This reduces to the arithmetic mean when $\rho = 1$ and is biased toward the time series maxima for larger values of ρ. We chose $\rho = 4$ to reduce the effect of zero abundances during the "inactive" periods. However, our results were robust to changes in ρ values. In our case, $t_0 = 0$, and t_1 is the end of the simulation.

S1.3 Local species persistence and biomass in single communities

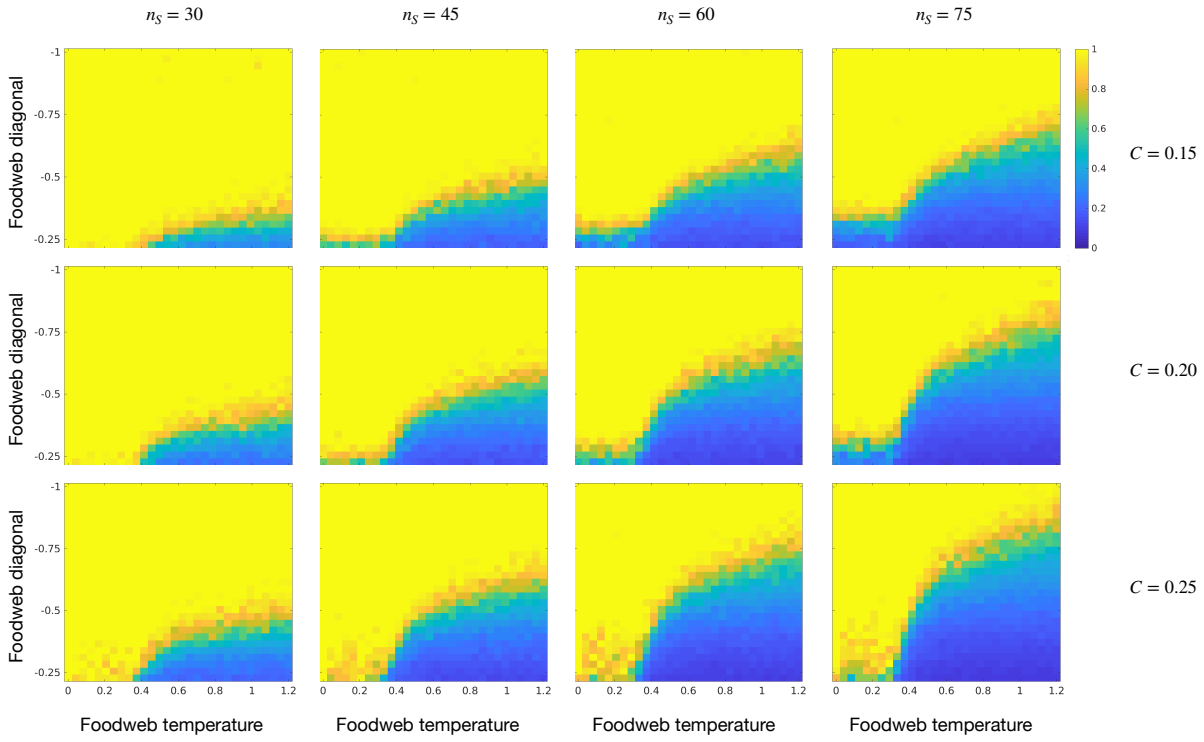

Fig. S2. Species persistence $\mathcal{P}$ in a single local community with colonization from a regional pool, as a function of foodweb diagonal values (opposite of intensity of self-regulation) and foodweb temperature values (inverse of trophic coherence) for a gradient of richness n_S and connectance C of the species pool. Each cell value shows the mean of 50 replicates.

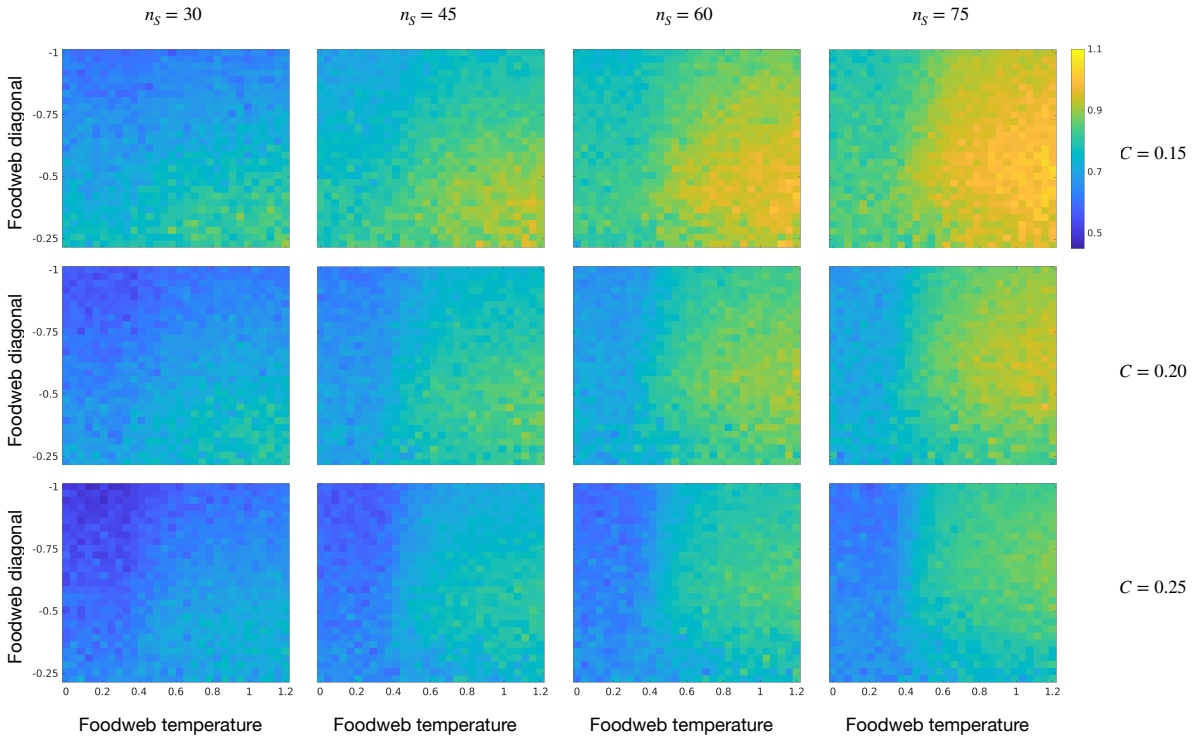

Fig. S3. Species biomass $\mathcal{B}$ (in $\log_{10}$) in a single local community with colonization from a regional pool, as a function of foodweb diagonal values (opposite of intensity of self-regulation) and foodweb temperature values (inverse of trophic coherence) for a gradient of richness n_S and connectance C of the species pool. Each cell value shows the mean of 50 replicates.

S1.4 Effects of local and regional stabilizing factors depending on landscape structure

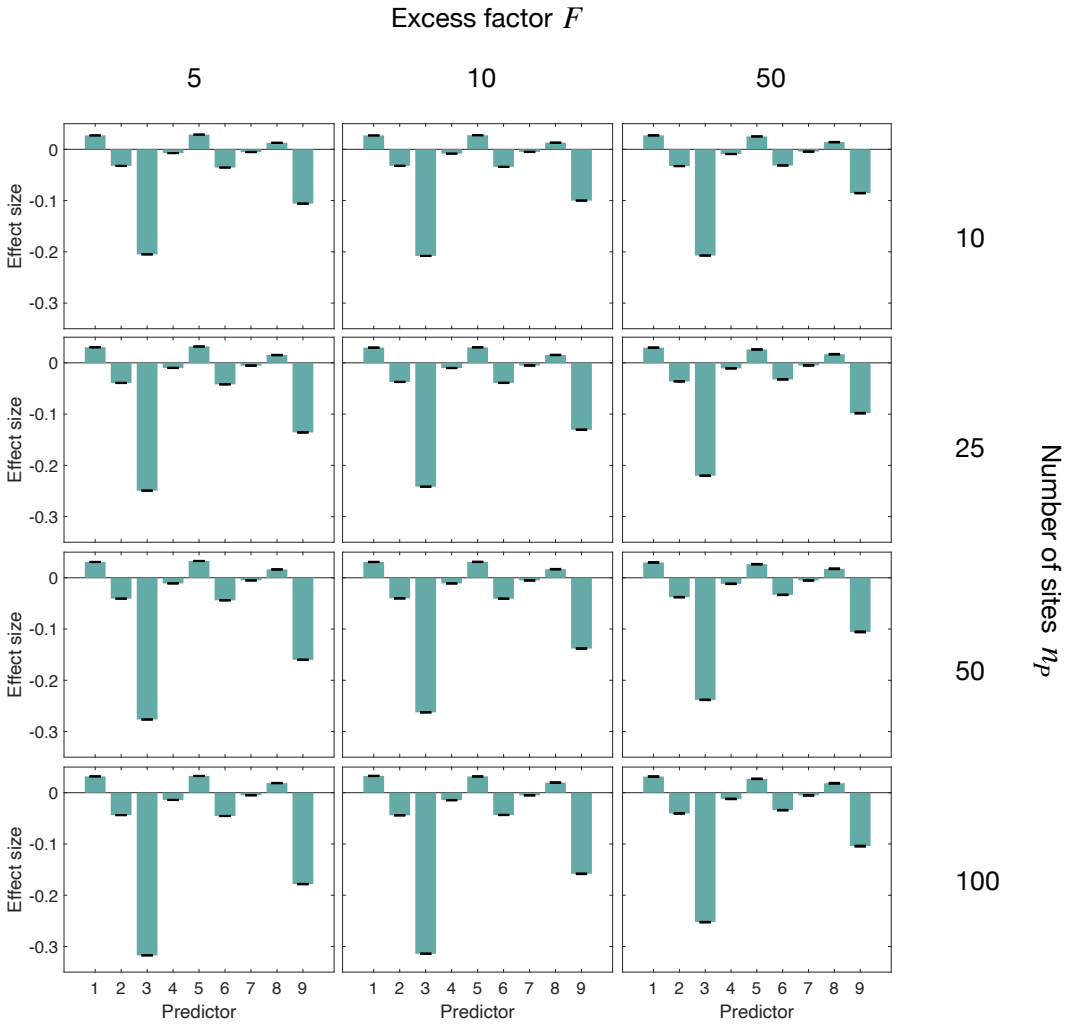

Fig. S4. Effect sizes on A-sensitivities of local species persistence $\mathcal{S}[\mathcal{P}_\alpha]$ in a gradient of number of sites n_P and excess factor F. Predictors are foodweb temperature T (1), self limitation λ (2), dispersal ability $\hat{a} = \log_{10} a$ (3), $T \cdot \lambda$ (4), $T \times \hat{a}$ (5), $\lambda \times \hat{a}$ (6), T^2 (7), λ^2 (8), and $\hat{a}^2$ (9). Foodweb parameters are $n_S = 45$ and $C = 0.2$

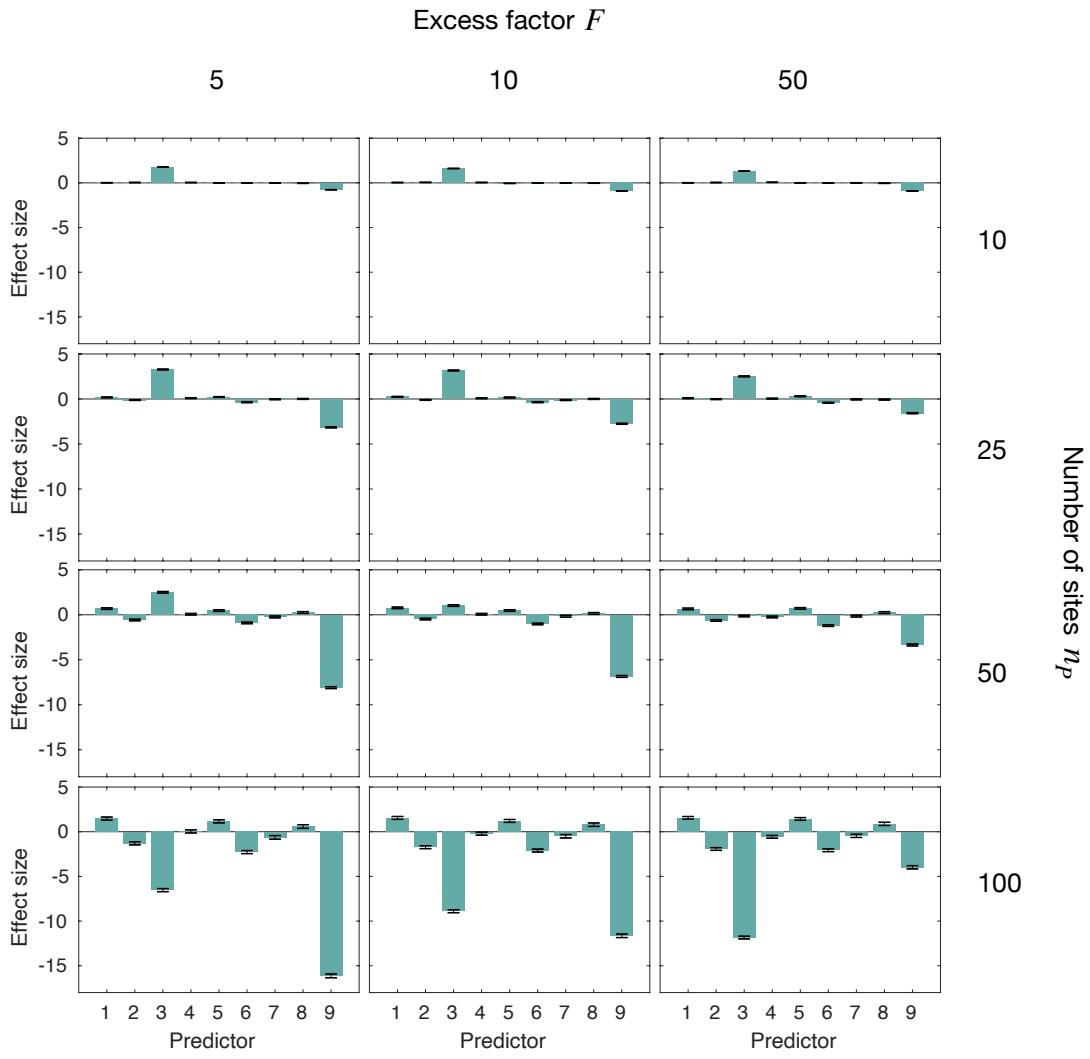

Fig. S5. Effect sizes on A-sensitivities of among-site dissimilarity in species persistence $\mathcal{S}[\mathcal{P}_\beta]$ in a gradient of number of sites n_P and excess factor F. Predictors are foodweb temperature T (1), self limitation λ (2), dispersal ability $\hat{a} = \log_{10} a$ (3), $T \cdot \lambda$ (4), $T \times \hat{a}$ (5), $\lambda \times \hat{a}$ (6), T^2 (7), λ^2 (8), and $\hat{a}^2$ (9). Foodweb parameters are $n_S = 45$ and $C = 0.2$

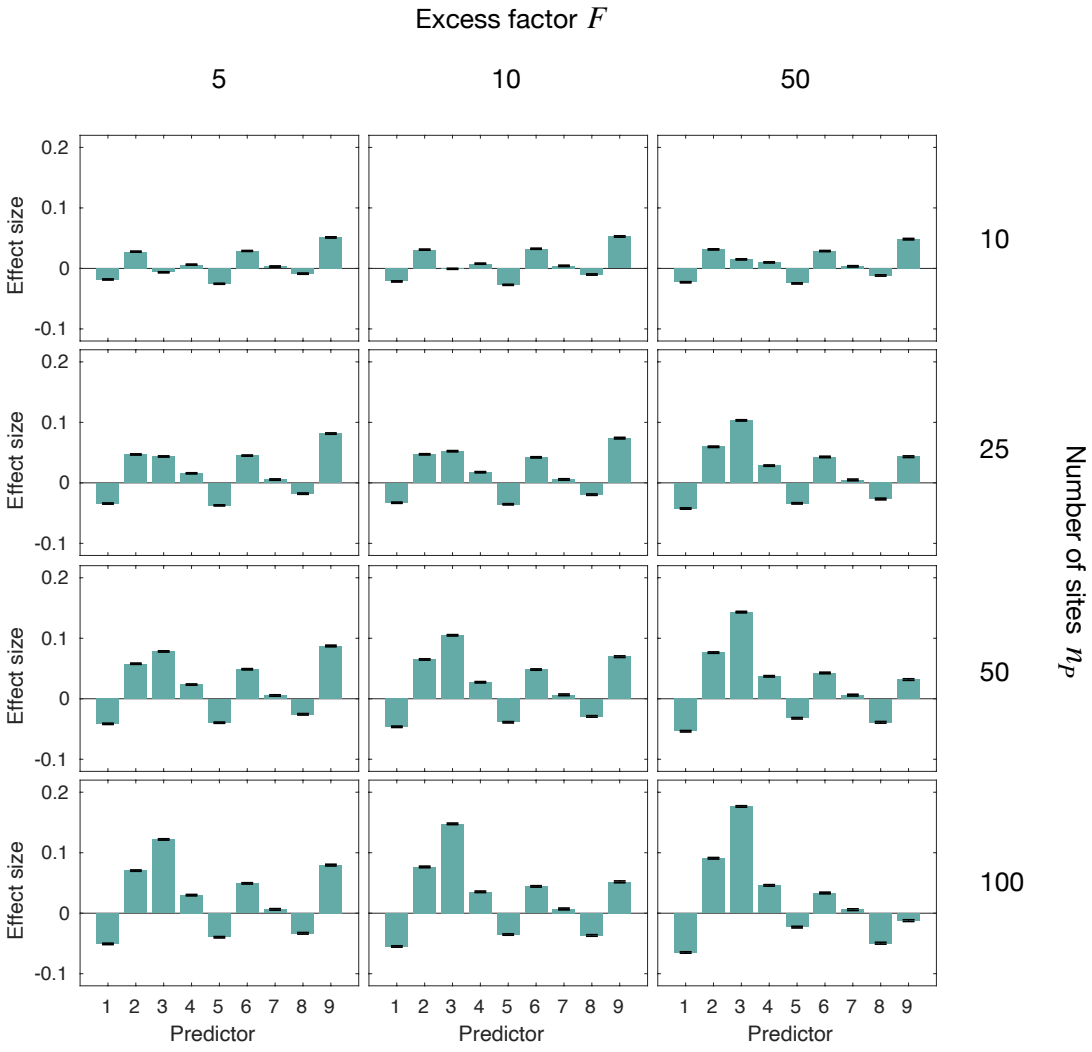

Fig. S6. Effect sizes on A-sensitivities of regional species persistence $\mathcal{S}[\mathcal{P}_\gamma]$ in a gradient of number of sites n_P and excess factor F. Predictors are foodweb temperature T (1), self limitation λ (2), dispersal ability $\hat{a} = \log_{10} a$ (3), $T \cdot \lambda$ (4), $T \times \hat{a}$ (5), $\lambda \times \hat{a}$ (6), T^2 (7), λ^2 (8), and $\hat{a}^2$ (9). Foodweb parameters are $n_S = 45$ and $C = 0.2$

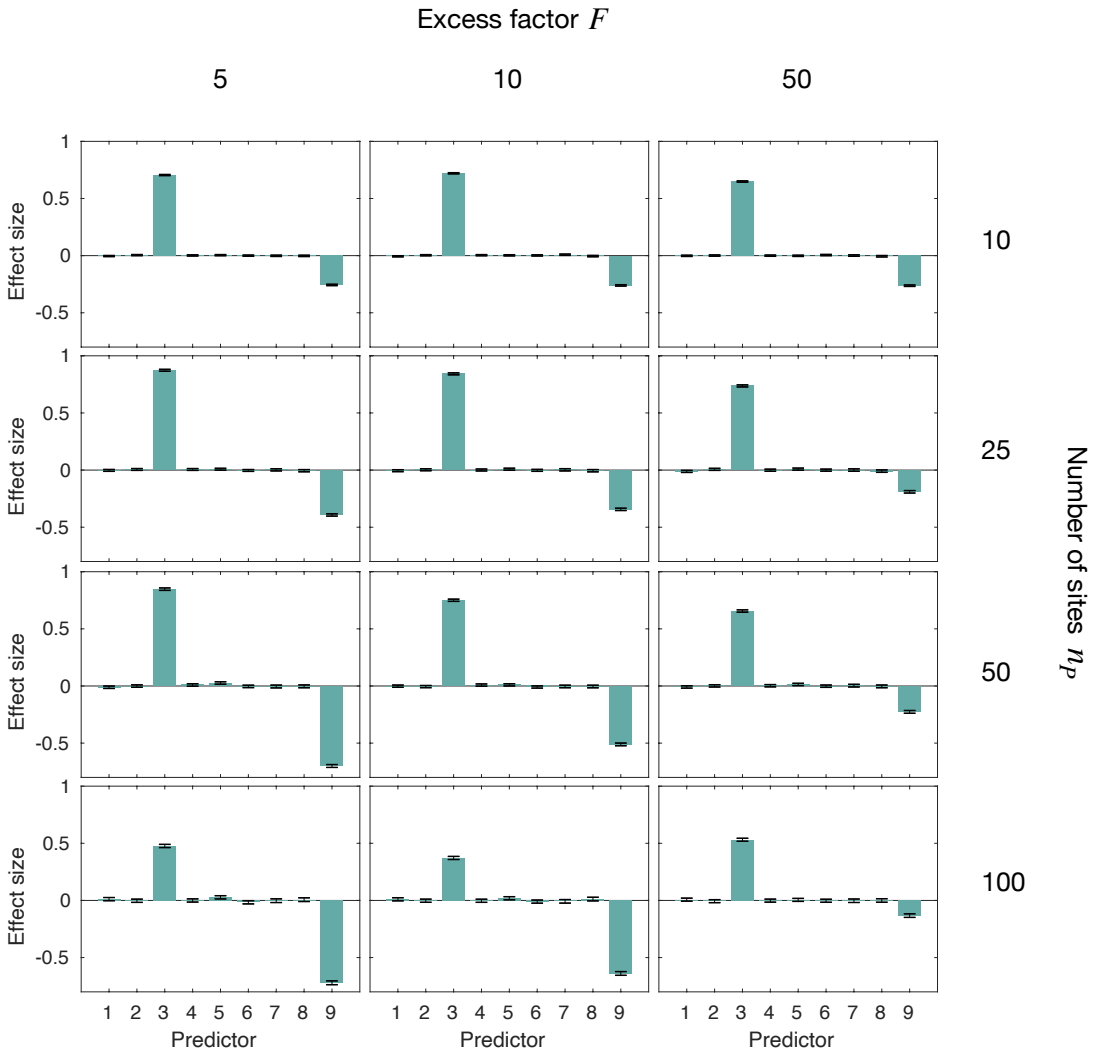

Fig. S7. Effect sizes on A-sensitivities of among-site dissimilarity in community biomass $\mathcal{S}[\mathcal{B}_\beta]$ in a gradient of number of sites n_P and excess factor F. Predictors are foodweb temperature T (1), self limitation λ (2), dispersal ability $\hat{a} = \log_{10} a$ (3), $T \cdot \lambda$ (4), $T \times \hat{a}$ (5), $\lambda \times \hat{a}$ (6), T^2 (7), λ^2 (8), and $\hat{a}^2$ (9). Foodweb parameters are $n_S = 45$ and $C = 0.2$

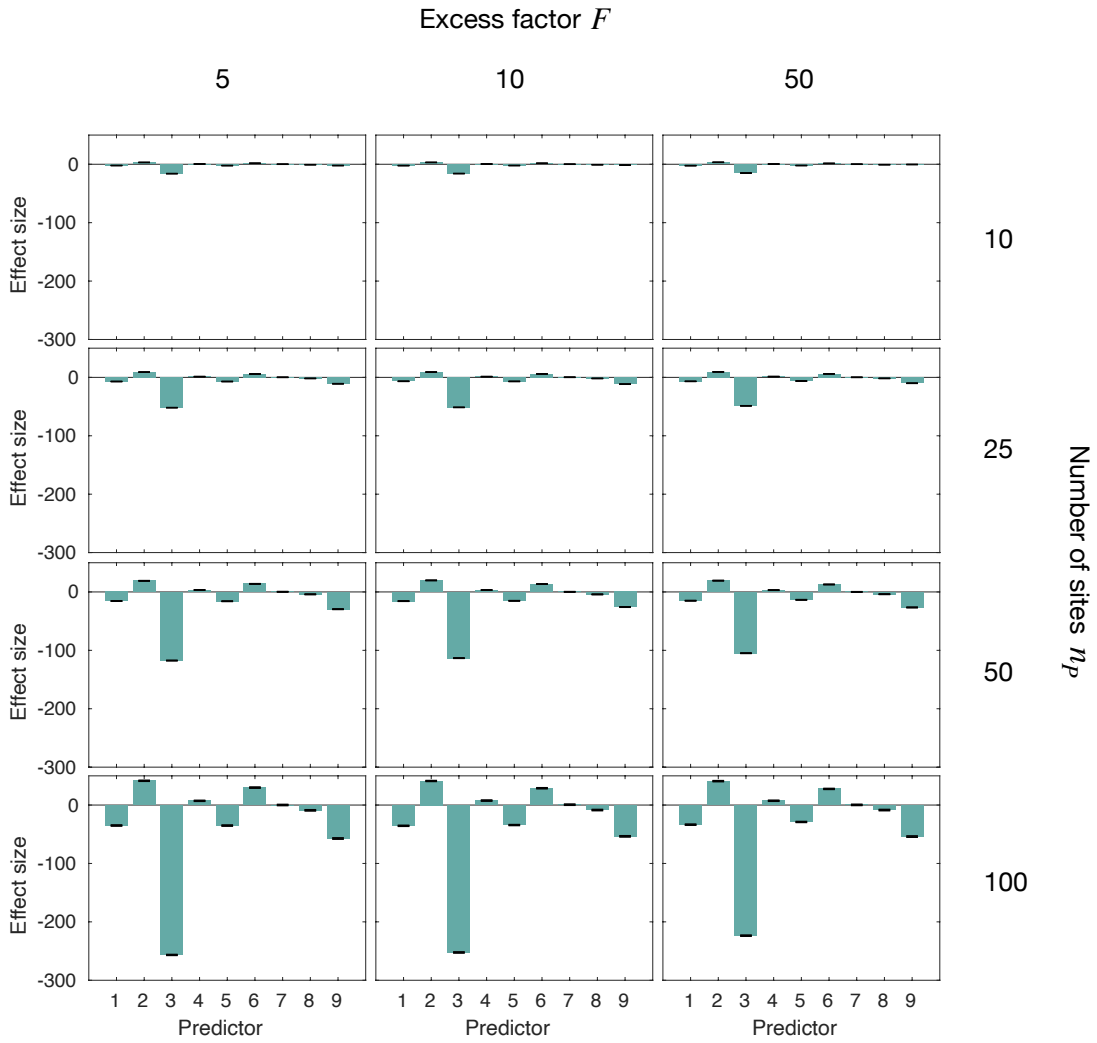

Fig. S8. Effect sizes on A-sensitivities of regional biomass $\mathcal{S}[\mathcal{B}_\gamma]$ in a gradient of number of sites n_P and excess factor F. Predictors are foodweb temperature T (1), self limitation λ (2), dispersal ability $\hat{a} = \log_{10} a$ (3), $T \cdot \lambda$ (4), $T \times \hat{a}$ (5), $\lambda \times \hat{a}$ (6), T^2 (7), λ^2 (8), and $\hat{a}^2$ (9). Foodweb parameters are $n_S = 45$ and $C = 0.2$

S1.5 Effects of local and regional stabilizing factors depending on foodweb topology

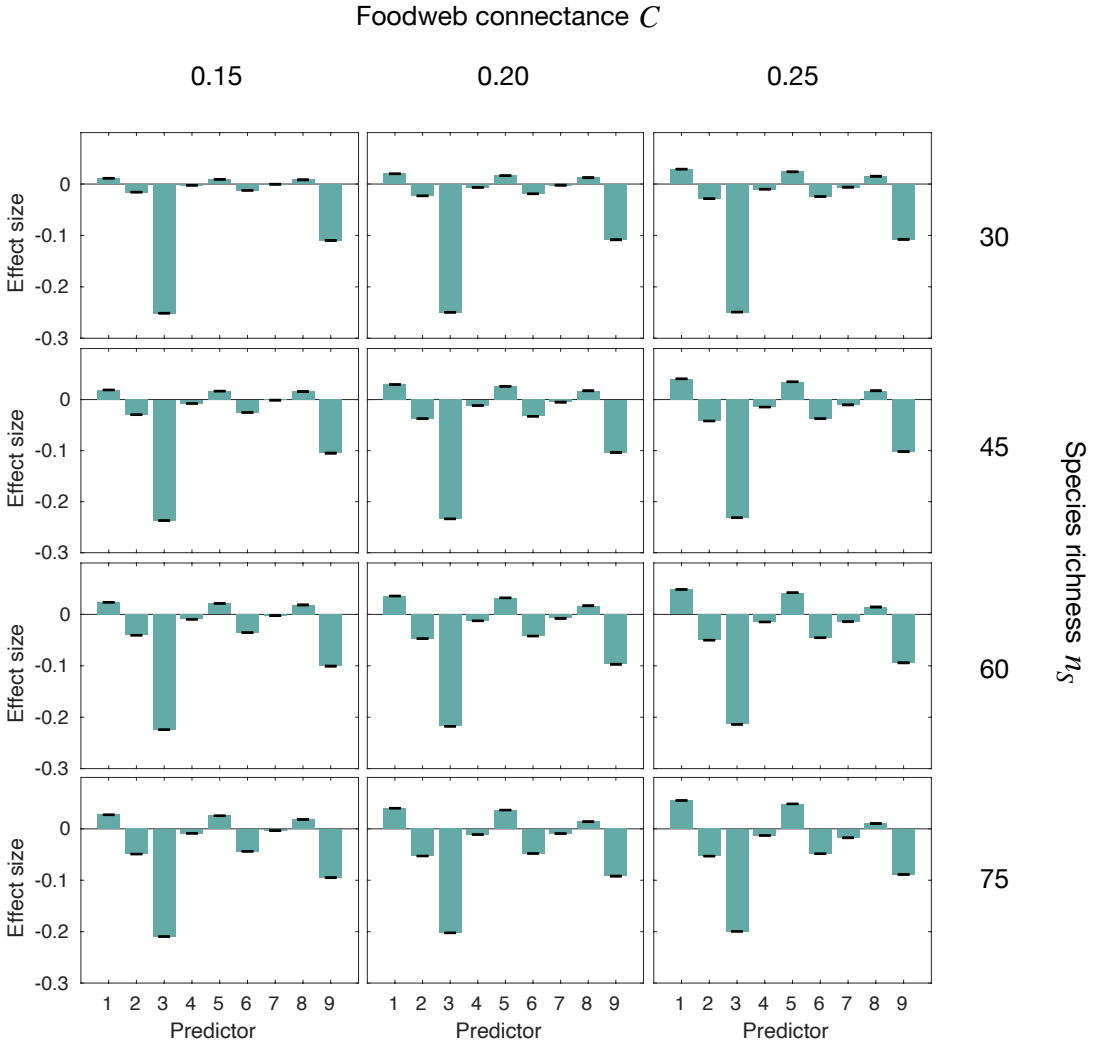

Fig. S9. Effect sizes on A-sensitivities of local species persistence $\mathcal{S}[\mathcal{P}_\alpha]$ in a gradient of foodweb connectance C and species richness n_S in the regional pool. Predictors are foodweb temperature T (1), self limitation λ (2), dispersal ability $\hat{a} = \log_{10} a$ (3), $T \cdot \lambda$ (4), $T \times \hat{a}$ (5), $\lambda \times \hat{a}$ (6), T^2 (7), λ^2 (8), and $\hat{a}^2$ (9). Landscape parameters are $n_P = 50$ and $F = 50$

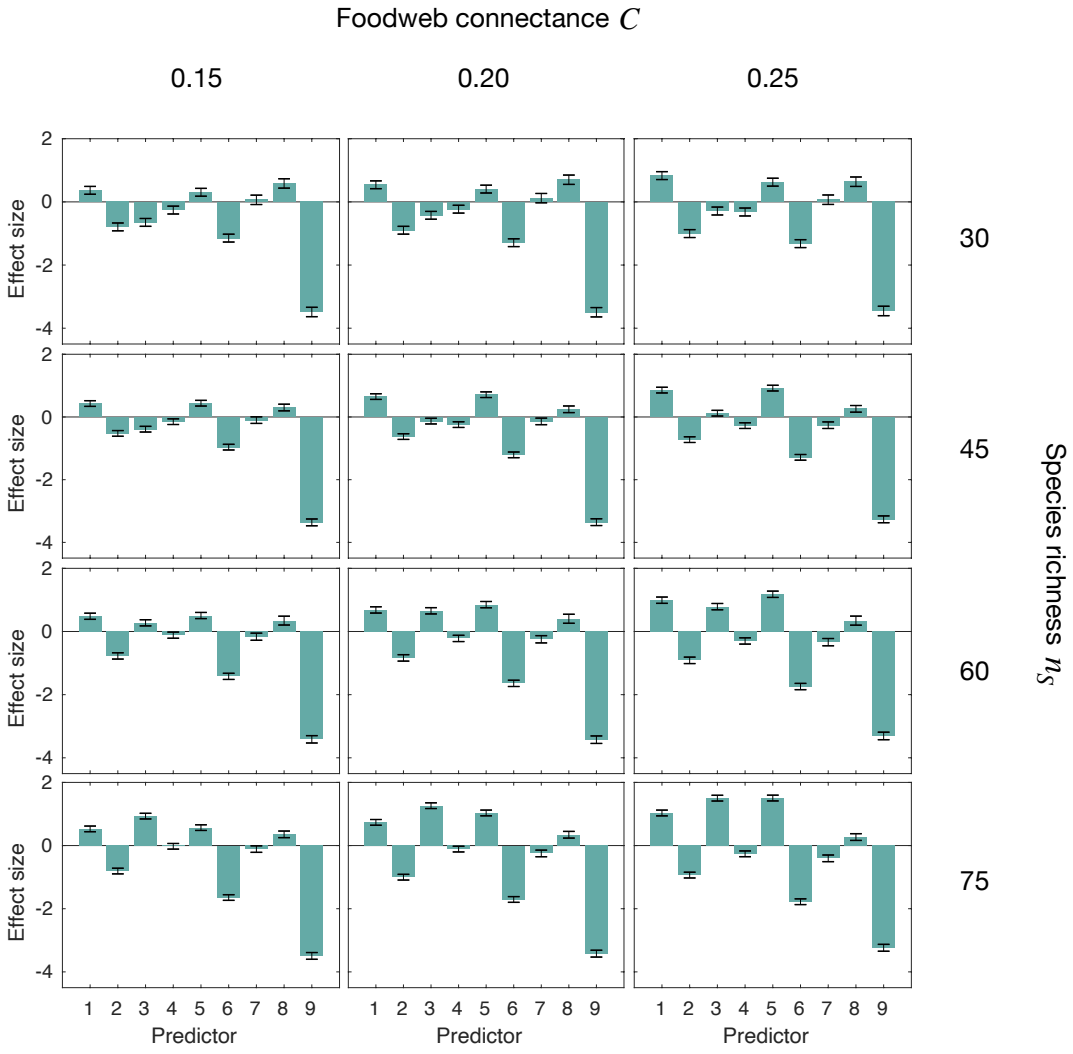

Fig. S10. Effect sizes on A-sensitivities of among-site dissimilarity in species persistence $\mathcal{S}[\mathcal{P}_\beta]$ in a gradient of foodweb connectance C and species richness n_S in the regional pool. Predictors are foodweb temperature T (1), self limitation λ (2), dispersal ability $\hat{a} = \log_{10} a$ (3), $T \cdot \lambda$ (4), $T \times \hat{a}$ (5), $\lambda \times \hat{a}$ (6), T^2 (7), λ^2 (8), and $\hat{a}^2$ (9). Landscape parameters are $n_P = 50$ and $F = 50$

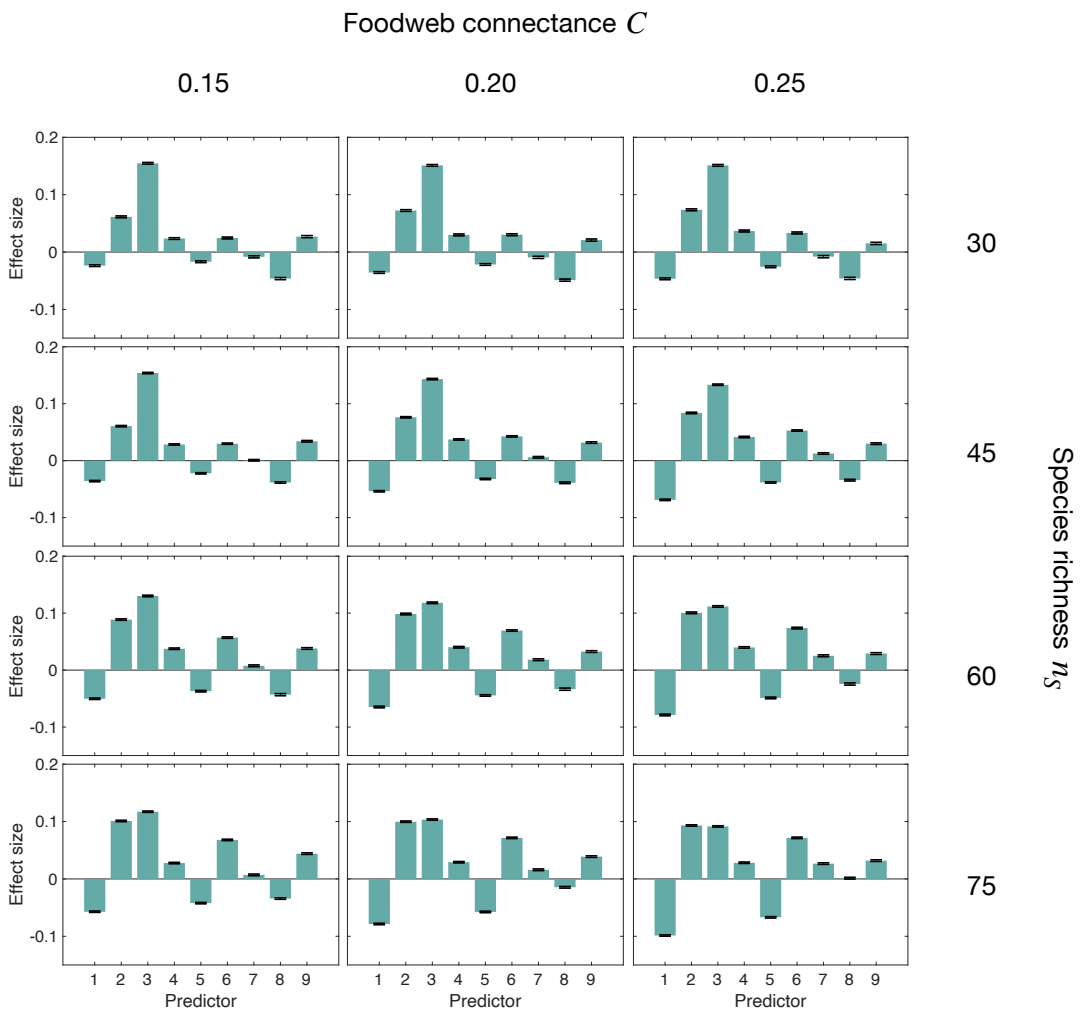

Fig. S11. Effect sizes on A-sensitivities of regional species persistence $\mathcal{S}[\mathcal{P}_\gamma]$ in a gradient of foodweb connectance C and species richness n_S in the regional pool. Predictors are foodweb temperature T (1), self limitation λ (2), dispersal ability $\hat{a} = \log_{10} a$ (3), $T \cdot \lambda$ (4), $T \times \hat{a}$ (5), $\lambda \times \hat{a}$ (6), T^2 (7), λ^2 (8), and $\hat{a}^2$ (9). Landscape parameters are $n_P = 50$ and $F = 50$

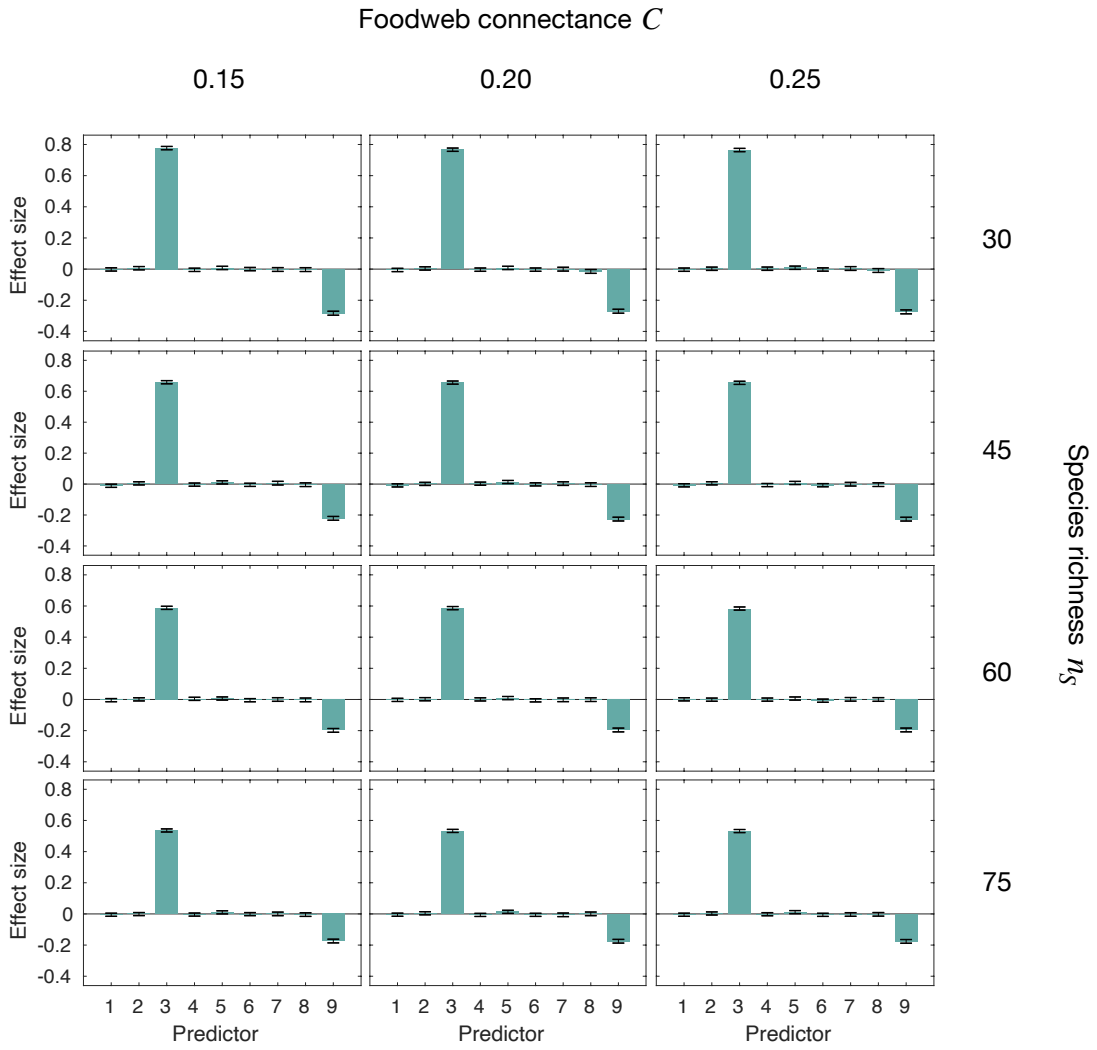

Fig. S12. Effect sizes on A-sensitivities of among-site dissimilarity in community biomass $\mathcal{S}[\mathcal{B}_\beta]$ in a gradient of foodweb connectance C and species richness n_S in the regional pool. Predictors are foodweb temperature T (1), self limitation λ (2), dispersal ability $\hat{a} = \log_{10} a$ (3), $T \cdot \lambda$ (4), $T \times \hat{a}$ (5), $\lambda \times \hat{a}$ (6), T^2 (7), λ^2 (8), and $\hat{a}^2$ (9). Landscape parameters are $n_P = 50$ and $F = 50$

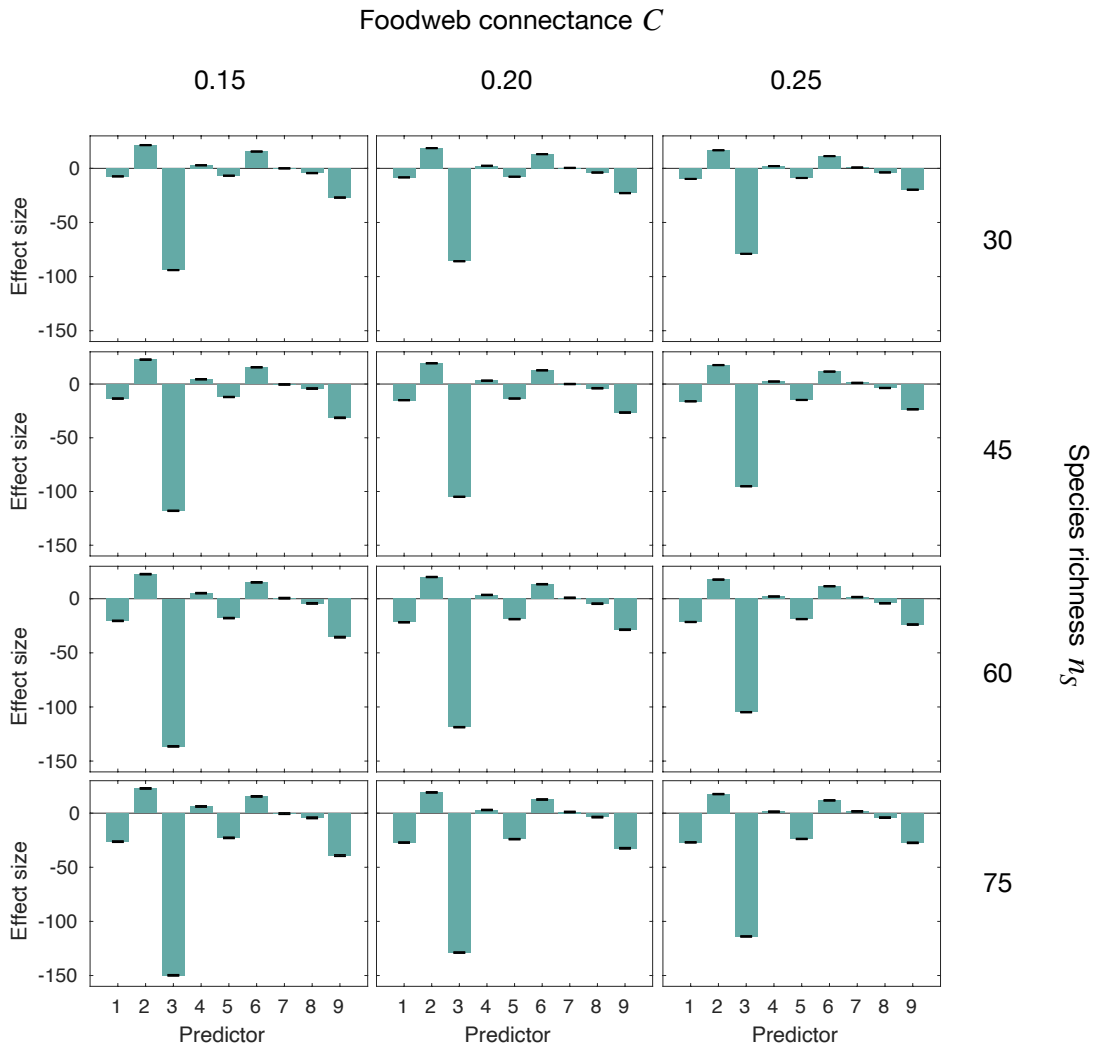

Fig. S13. Effect sizes on A-sensitivities of regional biomass $\mathcal{S}[\mathcal{B}_\gamma]$ in a gradient of foodweb connectance C and species richness n_S in the regional pool. Predictors are foodweb temperature T (1), self limitation λ (2), dispersal ability $\hat{a} = \log_{10} a$ (3), $T \cdot \lambda$ (4), $T \times \hat{a}$ (5), $\lambda \times \hat{a}$ (6), T^2 (7), λ^2 (8), and $\hat{a}^2$ (9). Landscape parameters are $n_P = 50$ and $F = 50$

S1.6 Sensitivities of $\mathcal{P}_\alpha$ and $\mathcal{P}_\gamma$

These figures depict metacommunity sensitivities as the changes in the distributions of $\mathcal{P}_\alpha$ and $\mathcal{P}_\gamma$ as sites' activation and deactivation asynchrony A increases from $A = 0$ to $A = 0.5$. For each parameter set, we run 50 replicates. However, for each data point, its coordinates represent the value of either $\mathcal{P}_\alpha$ or $\mathcal{P}_\gamma$ for the same foodweb and landscape but changing only A. The color of a dot represents the propensity to species persistence of a single local community (foodweb). The actual color depends on n_S, C, λ and T, and is looked up in Fig. S2. Thus, yellow/blue dots represent high/low local persistence. Note that stable-prone local communities tend to produce metacommunities with high regional persistences. This is apparent by the clustering of yellow circles close to large $\mathcal{P}_\gamma$ values. By contrast, the blue circles, representing unstable-prone local communities are scattered over a larger $\mathcal{P}_\gamma$ range. All simulations were carried out for landscapes with $n_C = 5$ and $F = 50$, and for a timelapse of 5 years. The magnitudes of metacommunity sensitivities are the vertical distances between each dot and the identity line. Positive sensitivities, i.e., when the response variable increases with landscape variability, are reached when the data points lie above the identity line, and vice versa.

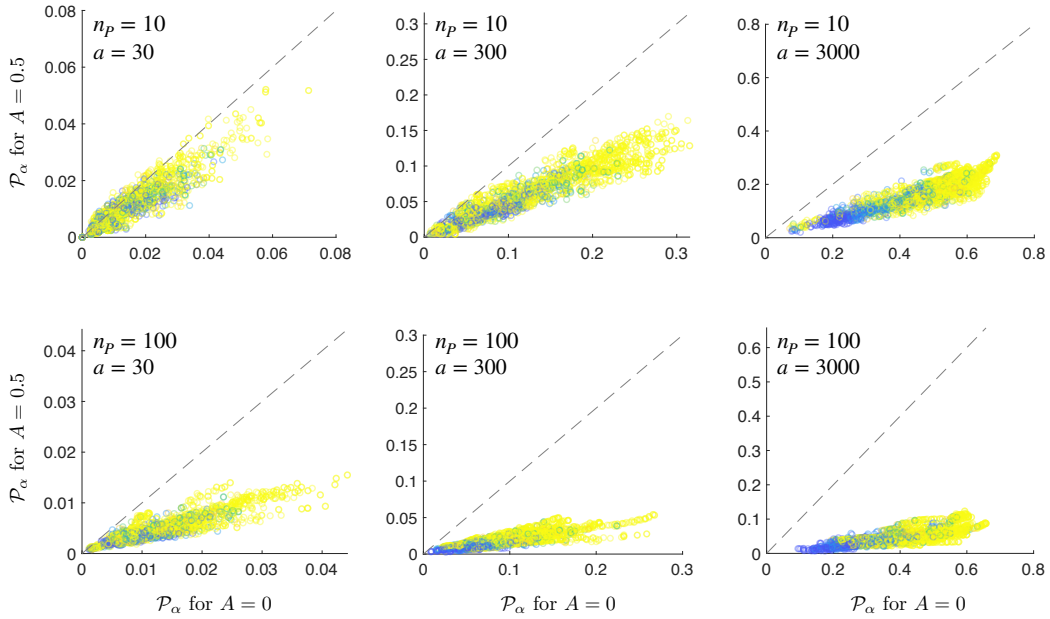

Fig. S14. $\mathcal{P}_\alpha$ for $A = 0$ versus $A = 0.5$ and three levels of dispersal ability (a). Foodweb parameters were $n_S = 45$ and $C = 0.2$. The top and bottom rows correspond to scattered/spread and dense landscapes respectively.

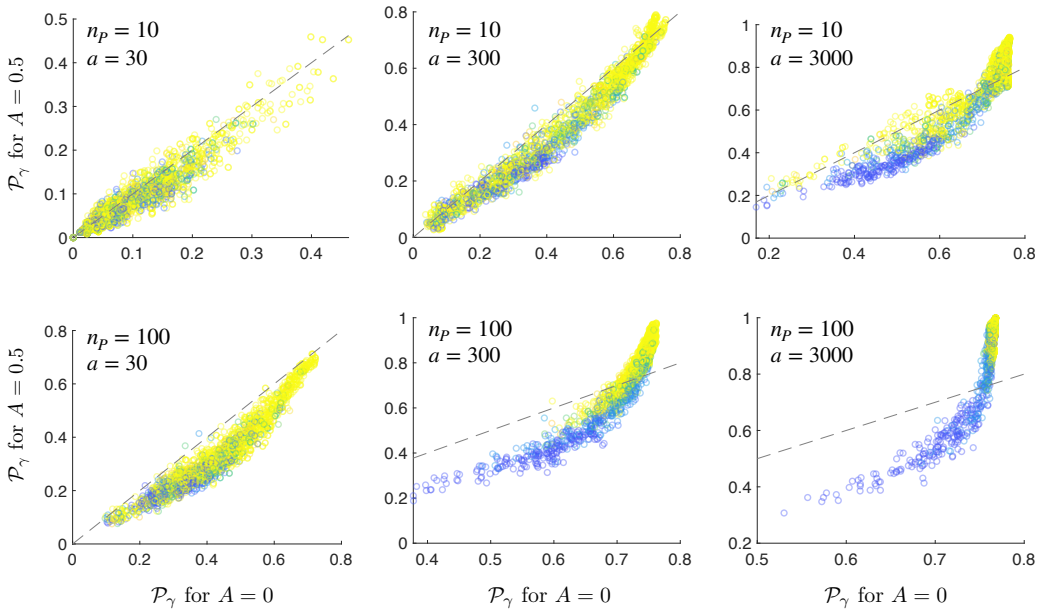

Fig. S15. $\mathcal{P}_\gamma$ for $A = 0$ versus $A = 0.5$ and three levels of dispersal ability (a). Foodweb parameters were $n_S = 45$ and $C = 0.2$. The top and bottom rows correspond to scattered/spread and dense landscapes respectively.

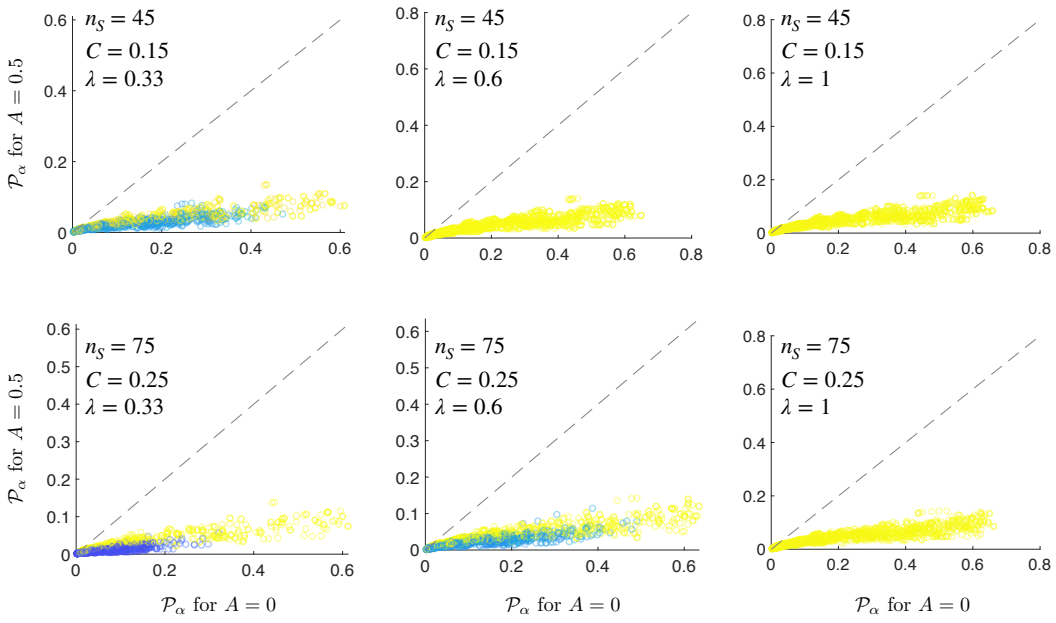

Fig. S16. $\mathcal{P}_\alpha$ for $A = 0$ versus $A = 0.5$ with $n_P = 50$ and three levels of self limitation (λ). The top and bottom rows correspond to simpler and more complex foodwebs respectively.

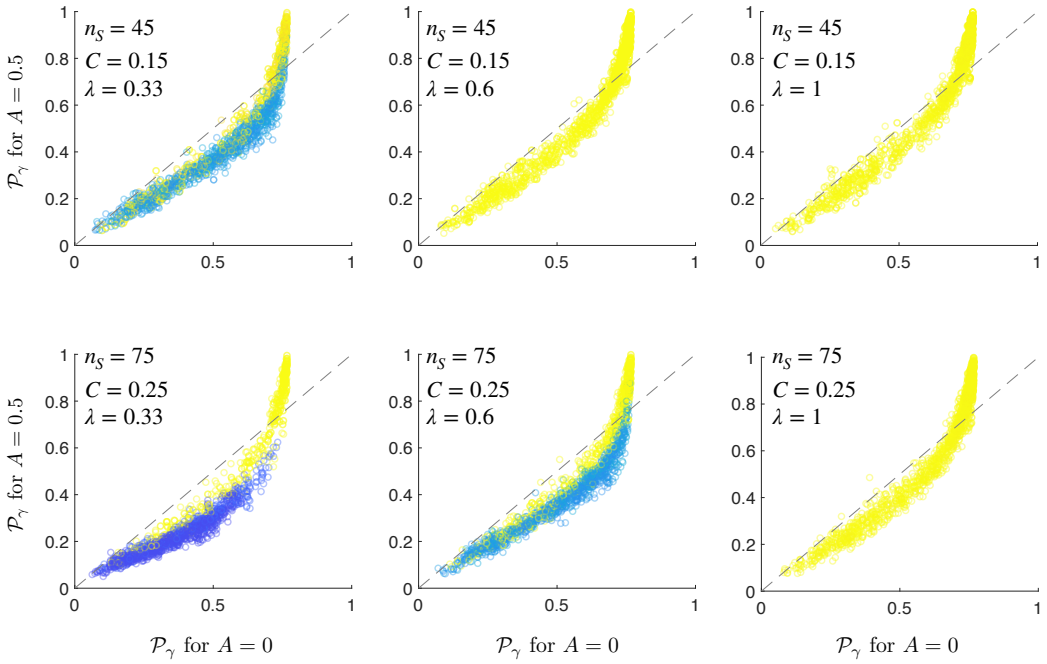

Fig. S17. $\mathcal{P}_\gamma$ for $A = 0$ versus $A = 0.5$ with $n_P = 50$ and three levels of self limitation (λ). The top and bottom rows correspond to simpler and more complex foodwebs respectively.

S1.7 Star experiment

This experiment simulated both stable-prone and unstable-prone local communities, on 10-point star landscapes. We used landscapes in which either all points or only three points can become active, mimicking low and high A values respectively. With higher A values, each temporal snapshot of the landscape graph turns sparser, thus implying fewer routes for dispersal among patches, which we approximate by allowing only three sites to be "active."

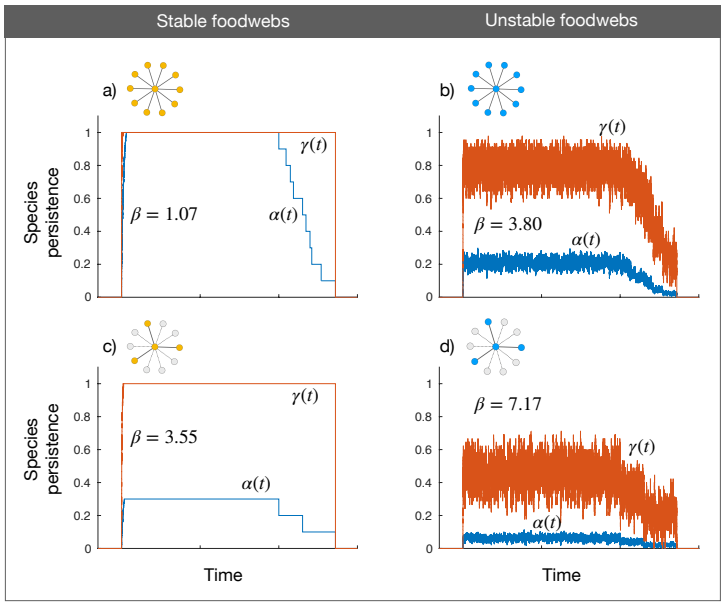

Fig. S18. Time series of α (blue lines) and γ (red lines) diversity (species persistence) over a single simulated year, of multitrophic metacommunities on an idealized landscape of a 10-point star topology. The central site is the mainland. The time average of β diversity is shown within each plot. Parameters values are $a = 3000$, $n_S = 45$, $C = 0.2$. Plots a) and c) show the dynamics of stable communities ($T = 0$, $\lambda = 0.33$). Plots b) and d) show the dynamics of unstable communities ($T = 1$, $\lambda = 0.33$). In plots a) and b) all points (sites) are available for dispersal, representing highly synchronous landscapes. In plots c) and d) only 3 out of 10 points are available for dispersal, representing highly asynchronous landscapes.

For stable-prone local communities, all colonization attempts are successful and do not cause secondary extinctions. Thus, for sufficiently large values of a, we can assume that all active sites contain the full set of species. In this scenario, both $\mathcal{P}_\alpha$ and $\mathcal{P}_\gamma$ are maximal, while $\mathcal{P}_\beta$ is minimal. Increasing A (from Fig. S18a to c) reduces $\mathcal{P}_\alpha$ simply by reducing the number of active sites. Conversely, if local communities are unstable-prone, two relevant competing processes take place. The first one includes successful colonization events that do not cause secondary extinctions. This process increases $\mathcal{P}_\alpha$ due to the direct introduction of a new species in the recipient community. In the second one, colonization attempts result in secondary extinctions, leading to reductions in $\mathcal{P}_\alpha$. The temporal alternation between these two processes causes the oscillations depicted in Figs. S18b and d and prevents $\mathcal{P}_\alpha$ and $\mathcal{P}_\gamma$ from always reaching their maximum possible values. For $A = 0$, $\mathcal{P}_\alpha$ attains low values because local instability hampers successful colonization events without secondary species extinctions. However, we do not observe a corresponding reduction in $\mathcal{P}_\gamma$, which shows there is a high among-site dissimilarity ($\mathcal{P}_\beta$). Increasing A (from Fig. S18b to d) reduces $\mathcal{P}_\alpha$ because of reduction in active sites. However, the reduction in $\mathcal{P}_\gamma$ is relatively small because of the large values of $\mathcal{P}_\beta$. This small experiment captures the interplay between the LSFs and landscape asynchrony and how it shapes the biodiversity patterns observed in the full model.